chapter 6

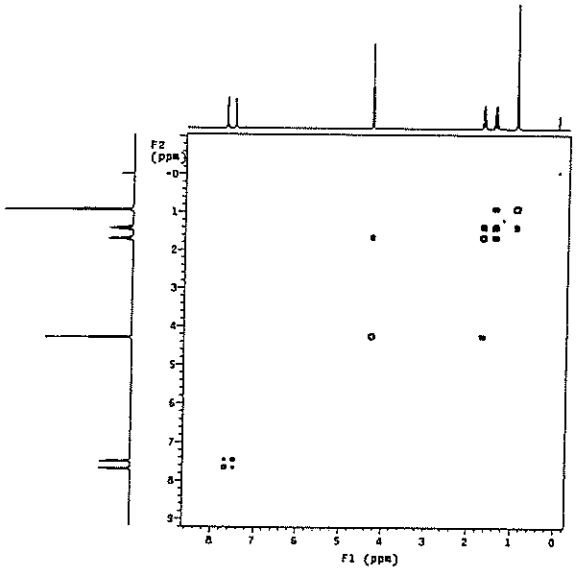

Two-Dimensional NMR

NMR always has been multidimensional. In addition to frequency and intensity, which serve as the axes of the standard one-dimensional spectrum, reaction rates and relaxation times have provided additional dimensions, often presented as stacked plots (see Figures 2-33 and 5-2). The second dimension of modern NMR, however, refers to an additional frequency axis. This concept was first suggested in a lecture by Jeener in 1971 and reached wide application in the 1980s when instrumentation caught up with theory. In terms of structure, we can think of the first frequency dimension as the traditional characterization of nuclei in terms of chemical shifts and couplings. In the second frequency dimension, we further consider magnetic interactions between nuclei through structural connectivity, spatial proximity, or kinetic interchange.

6-1 PROTON–PROTON CORRELATION THROUGH COUPLING

In the single-pulse experiments described up to this point, a 90° pulse is followed by a period of time during which the free induction decay is acquired (Figure 6-1a). Fourier transformation of the time-dependent magnetic information into a frequency dimension provides the familiar spectrum of δ values, now to be called a one-dimensional (1D) spectrum. If the 90° pulse is preceded by another 90° pulse (Figure 6-1b), useful relationships between spins can evolve prior to acquisition. Figure 6-2 illustrates what happens in terms of magnetization vectors.

Consider a sample that contains only one type of nucleus without any coupling partners, for example the ^{1}H spectrum of tetramethylsilane. Although the final result of the particular experiment we are about to describe may seem trivial or even pointless at first, it will take on fuller meaning when we introduce relationships with other nuclei. The isolated nucleus of Figure 6-2 begins with magnetization aligned along the z axis (a), and then along the y axis after application of the 90° pulse (b). If the coordinate system rotates at the carrier frequency and the nucleus resonates at a slightly higher frequency, the spin vector picture beings to evolve. After a short amount of time, the vector M moves to a new position in the xy plane, for example in (c). We ignore longitudinal

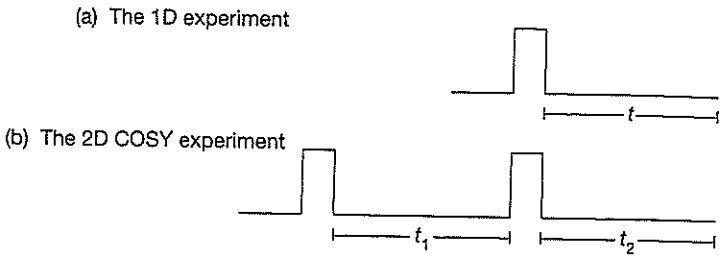

Figure 6-1 The pulse arrangements for a single cycle of one-dimensional NMR spectroscopy (upper) and for two-dimensional NMR correlation spectroscopy (COSY) (lower). In this diagram each pulse is 90°. Data are acquired during the time period t_2 in the 2D experiment.

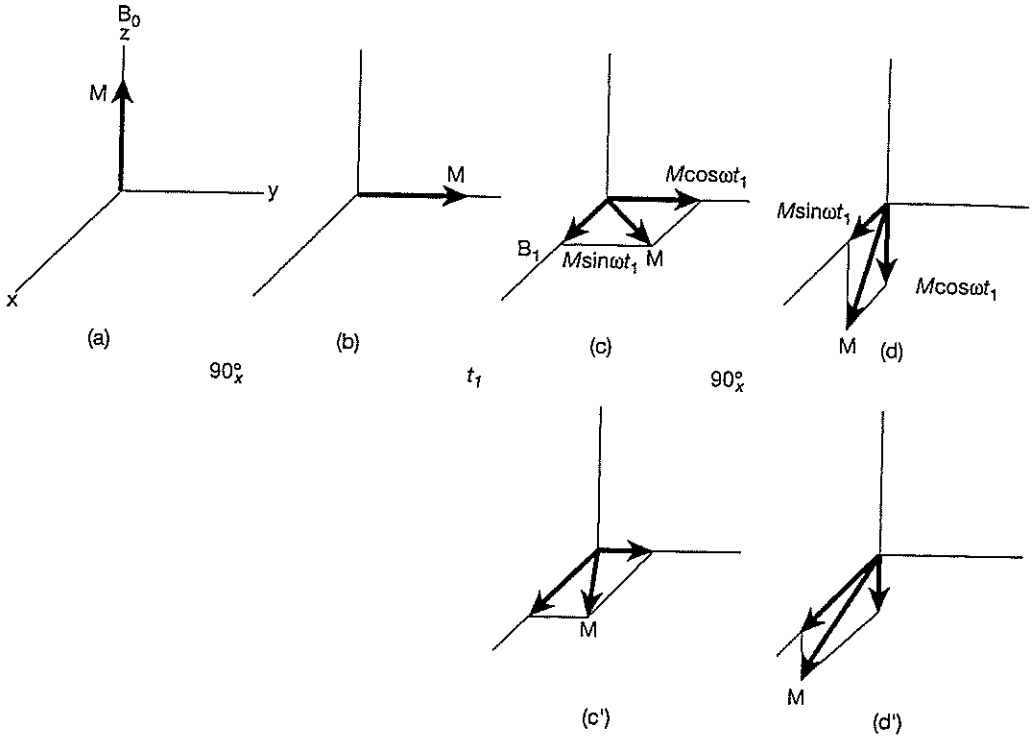

Figure 6-2 The pulse sequence for the COSY experiment. For (c') the magnetization M is allowed to evolve a longer time from (b) than for (c) before the final 90°_x pulse is applied to give (d').

relaxation (T_1) to simplify the drawings. The evolving magnetization vector may be decomposed into a y component ($M_y = M\cos\omega t_1$) and an x component ($M_x = M\sin\omega t_1$), in which ω is the difference between the frequency of the carrier and of the resonating nucleus and t_1 is the time elapsed since the 90° pulse.

If at this point the second 90° pulse of Figure 6-1b is applied, again along the x axis, the result is different for the two illustrated magnetization components (Figure 6-2d). The x component is unaffected, but the y component is transferred to the negative z axis. If observation is in the xy plane, the only detectable part of the magnetization is M_x. This quantity appears as a free induction decay during the time period t_2 after the second pulse. Fourier transformation of the FID as a function of t_2 yields a signal at the resonance frequency (ν_A). The intensity of this signal is determined by the quantity $M\sin\omega t_1$. The use of the subscripts is necessary to distinguish the evolution period t_1 from the acquisition period t_2 (Figure 6-1b). If t_1 is relatively short, M_x ($= M\sin\omega t_1$) is small, little x magnetization has developed (d), and the peak is small. A slightly longer value of t_1 yields a larger x component (c' and d') as $M\sin\omega t_1$ grows.

Figure 6-3 shows the result of a whole series of such experiments, with buildup of M_x ($= M\sin\omega t_1$) as t_1 increases, reaching a maximum when the spin vector M is lined up

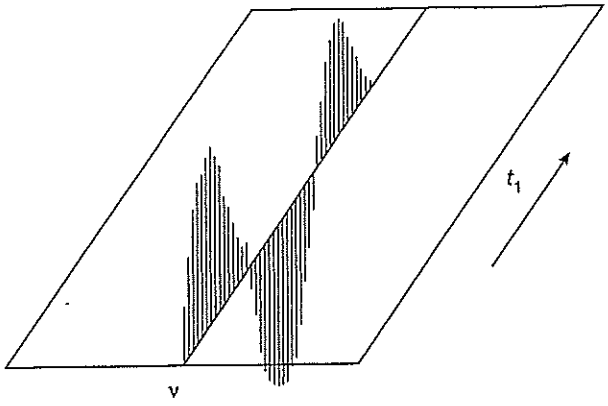

Figure 6-3 The middle diagonal serves as the baseline for a series of ^1H spectra of chloroform according to the COSY pulse sequence for a series of values of t_1. Each peak is one period of 90°–t_1–90° followed by Fourier transformation during t_2 of Figure 6-1. Fourier transformation in the t_1 dimension has not been carried out.

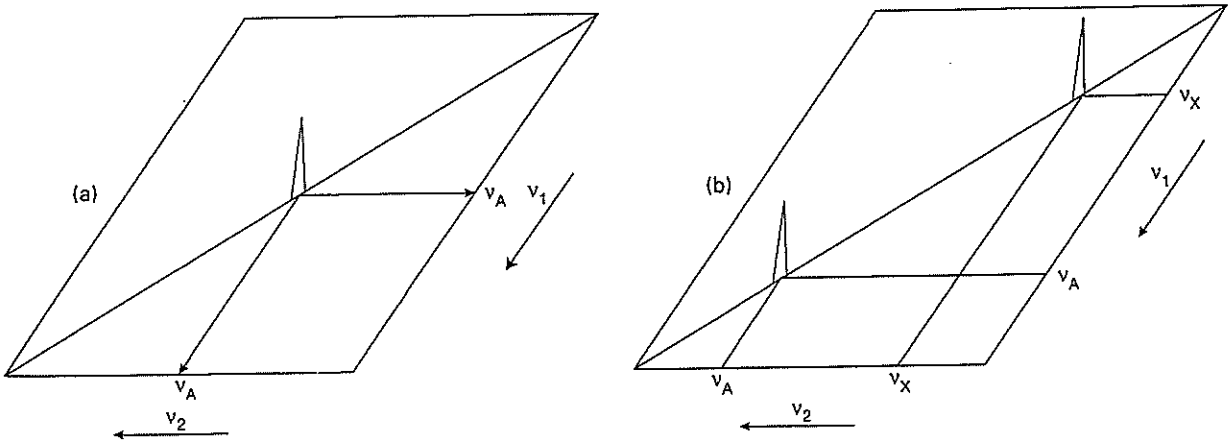

Figure 6-4 (a) The result of the COSY experiment after double Fourier transformation for a single, isolated nucleus such as that in Figure 6-3. (b) The result of the COSY experiment for two uncoupled nuclei.

along the x axis. The peak height then decreases as the vector moves to the left of the x axis, reaching zero intensity when it is lined up along the negative y axis. As it passes behind the y axis, the intensity becomes negative, reaching a negative maximum when the vector is aligned along the $-x$ axis. This negative maximum would be slightly smaller than the initial positive maximum because of T_2 relaxation. It is clear from Figure 6-3 that this family of experiments generates a sine curve when M_x is plotted as a function of t_1. Frequency (from Fourier transformation of t_2 to give ν_2) is along the horizontal dimension and the time t_1 is along the vertical dimension. The type of data generated from stepping t_1 in this fashion in fact comprises a free induction decay that also may be Fourier transformed. Because the frequency ω represented by the sine curve in t_1 is the same as the frequency from the initial Fourier transformation in t_2, the result of the second Fourier transformation is a single peak at the coordinates (ν_A,ν_A) when plotted in two frequency dimensions (Figure 6-4a). This is the trivial result previously alluded to.

The utility of this experiment becomes evident when two coupled nuclei are treated in this fashion. Two uncoupled nuclei yield the trivial result of two peaks respectively at (ν_A,ν_A) and $\nu_X,\nu_X)$, as in Figure 6-4b. These peaks are on the diagonal of the two-dimensional representation. Satisfying complications arise when the two nuclei are coupled. Figure 6-5 illustrates the possible spin states for nuclei A and X, as for example the

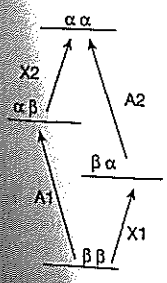

Figure 6-5

alkenic protons in β-chloroacrylic acid, $ClCH{=}CHCO_2H$. The AX spectrum contains four peaks due to scalar *(J)* coupling. The diagram is intended to indicate the four different frequencies, from the highest (A1) to the lowest (X2). It is useful first to consider population perturbations during an old-style, one-dimensional selective decoupling CW experiment. Irradiation, for example, of only transition A1 tends to bring the αβ and ββ states closer together in population. Consequently, there is a direct effect on the intensities of the connected transitions X1 and X2, which propagates as a secondary effect on the intensity of the A2 transition. With respect to A1, X2 is called a *progressive transition* (going on to a higher spin state), X1 is called a *regressive transition,* and A2 is called a *parallel transition*..

In the pulse experiment, energy absorption at frequency A1 has similar effects, which bring about magnetization or population transfer. The first 90° pulse serves to label all the magnetization with the 1D frequencies during period t_1: A1, A2, X1, X2. The second 90° pulse results in a population inversion for any given transition (Figure 6-2d). This perturbation causes population changes in all connected transitions of the resonances to which the nucleus is coupled, and secondarily to parallel transitions. Part of the magnetization at frequency A1, for example, is transferred by the second pulse during period t_2 to each of the other three transitions. This transferred magnetization has a new frequency. Such transfers occur from all four of the transitions to each of the other three. Thus the magnetization observed at frequency A1 during t_2 contains components modulated at frequencies A2, X1, and X2. That portion of the magnetization, for example, that has frequency A1 during t_1, but frequency X2 during t_2, is observed as a peak off of the diagonal, at frequency (ν_{A1},ν_{X2}). In the absence of J couplings, the A and X transitions of Figure 6-5 are not connected and magnetization is not transferred.

Figures 6-6 and 6-7 are two representations of the two-dimensional experiment for β-chloroacrylic acid. In Figure 6-6 the stack representation contains several hundred complete 1D experiments, whose closely packed horizontal lines are barely distinguishable. On the diagonal from the lower left to the upper right (as drawn into the plots in Figure 6-4) are the four peaks that arise directly from resonance without magnetization transfer, that is, the components of magnetization that possess the same frequency in t_1 and t_2. These four peaks comprise the normal, four-peak 1D spectrum. All the peaks off of the diagonal represent magnetization transfer by scalar *(J)* coupling.

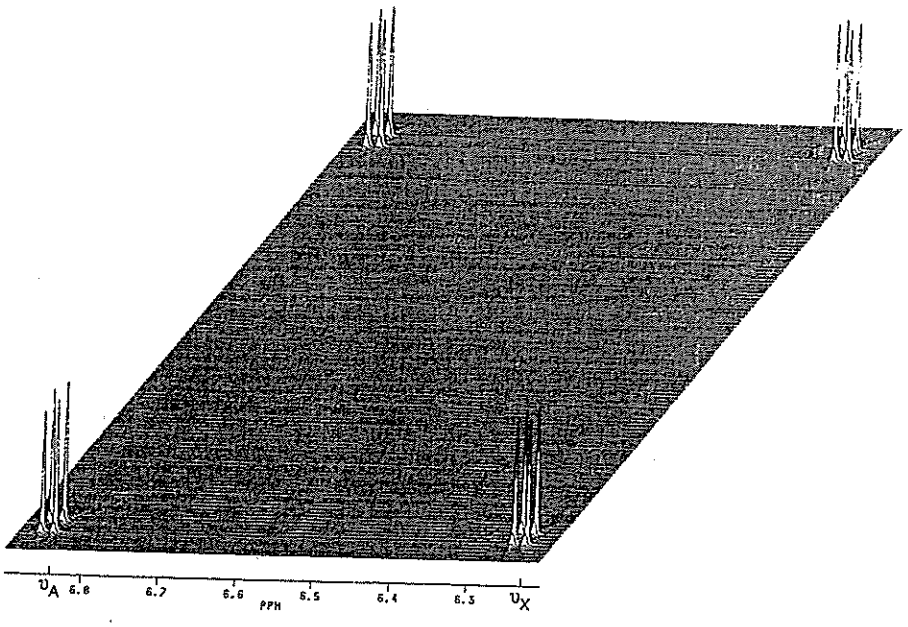

Figure 6-6 The stacked representation of the COSY experiment for two coupled nuclei (β-chloroacetic acid). (Reproduced from A.E. Derome, *Modern NMR Techniques for Chemistry Research,* Pergamon Press, Oxford, UK, 1987, p. 189.)

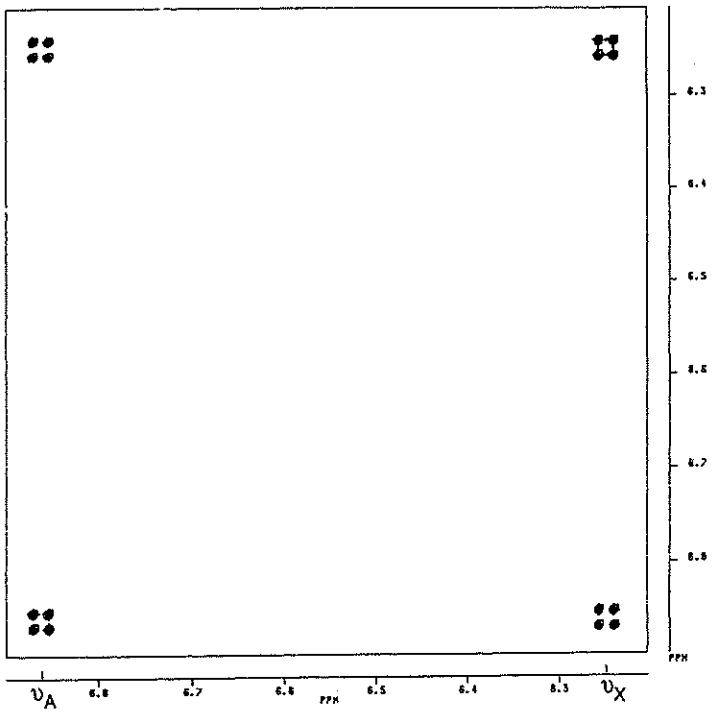

Figure 6-7 The contour representation of the COSY experiment for two coupled nuclei (β-chloroacetic acid). (Reproduced from A.E. Derome, *Modern NMR Techniques for Chemistry Research,* Pergamon Press, Oxford, UK, 1987, p. 191.)

For example, transfer between the parallel transitions A1 and A2 is found as symmetrical peaks just above and below the diagonal at the lower left. One peak represents transfer from A1 to A2 and the other from A2 to A1. Because of this reciprocal relationship, all off-diagonal peaks appear in pairs reflected across the diagonal. Normally, the off-diagonal peaks between parallel transitions are more nuisance than use and can be reduced or deleted by special techniques. The important information results from magnetization transfer between the A and the X nuclei, whose peaks are the clusters in the upper left and lower right of Figure 6-6, representing all the possible transfers between the A and X transitions: A1 to X1, X2 to A1, and so on, eight in total, including the mirror image pairs (A to X and X to A) on either side of the diagonal.

Figure 6-7 is the alternative *contour representation* of the same data, in which the distracting baselines are removed and only the peak bases remain, as if the spectator is viewing the spectrum from directly above it. By convention, the original diagonal usually is from lower left to upper right. The Jeener experiment commonly is given the semiacronym COSY, for **CO**rrelation **S**pectroscop**Y**. Since most 2D experiments involve spectral correlations, the name is not apt. Alternative terms such as 90° COSY, COSY90, H,H-COSY, or homonuclear HCOSY have been subsumed by public acceptance of the term COSY. The experiment itself has become an essential part of the analysis of complex proton spectra.

Figure 6-8 is the COSY experiment for the indicated annulene, from the work of H. Günther. The 1D spectrum is shown along both horizontal and vertical axes, and the resonances are labeled α, β, and A to F. The aromatic protons that are ortho and meta to the ring fusion provide an isolated spin system, and their coupling is represented by the off-diagonal (or cross) peak labeled α,β. The presence of a cross peak normally indicates that the protons giving the connected resonances on the diagonal are geminally or vicinally coupled. Long-range couplings do not usually provide significant cross peaks. Exceptions, however, can be expected, since long-range couplings can be large.

The COSY analysis of the remainder of the spectrum in Figure 6-8 provides the peak assignments and confirms the structure. Protons A and F are the only ones split by

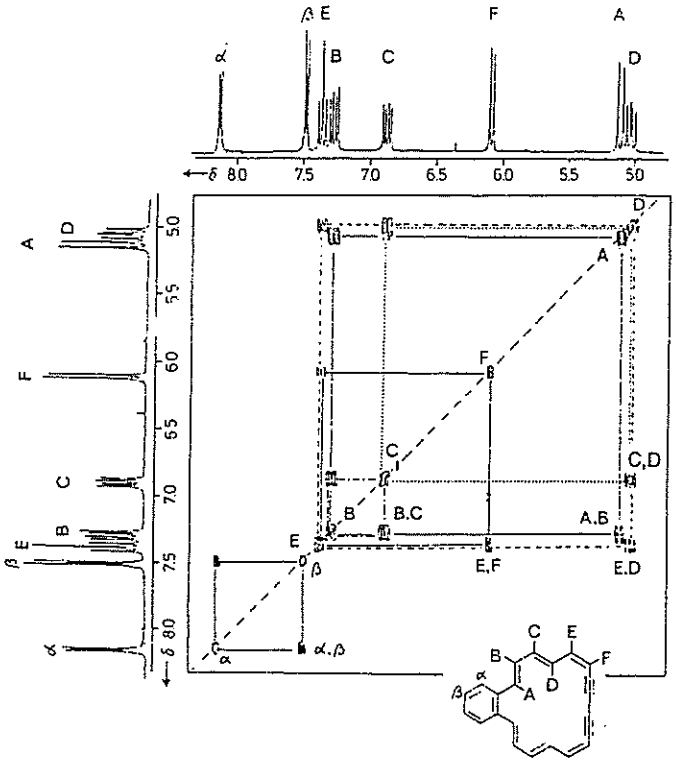

Figure 6-8 The COSY experiment for the illustrated annulene. (Reproduced from R. Benn and H. Günther, *Angew. Chem., Int. Ed. Engl.*, **22**, 350 [1983]).

a single neighbor. The coupling of A with B is trans and should be larger than the cis coupling between E and F. The two doublets then may be assigned as F (smaller coupling) at δ 6.1 and A (larger coupling) at δ 5.2. It usually is essential in a COSY analysis to be able to make an initial assignment through traditional considerations of chemical shifts and coupling constants (see Chapters 3 and 4). The COSY analysis then consists of moving from the known diagonal peak, to a cross peak, and back to the diagonal for the assignment of a new peak. Only A and F have single cross peaks (one coupling partner). All remaining resonances in the large ring have two cross peaks, which provide the means for assignment. We can start with either A or F. Dropping down from A leads to the cross peak A,B, and horizontal movement to the left leads to a diagonal peak and the assignment of proton B. The horizontal path passes through another cross peak, which must be between B and its other coupling partner, C. Moving up from B,C then leads to a diagonal peak and assignment of proton C. Horizontal movement to the right leads to the cross peak C,D, and return upward to the diagonal assigns proton D. Dropping back down from D and passing through C,D leads to the other cross peak from D, labeled E,D. Returning to the diagonal to the left assigns proton E and passes through the other cross peak from E, labeled E,F. Return upward from E,F to the diagonal completes the assignment with proton F.

A group at IBM has provided a useful example of a more complex COSY analysis with the tripeptide Pro-Leu-Gly **(6-1)**. The three carbonyl groups disrupt vicinal

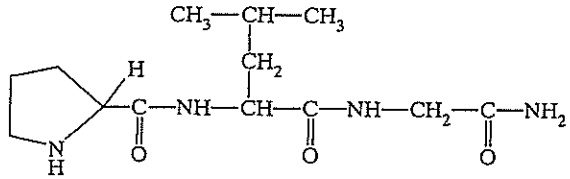

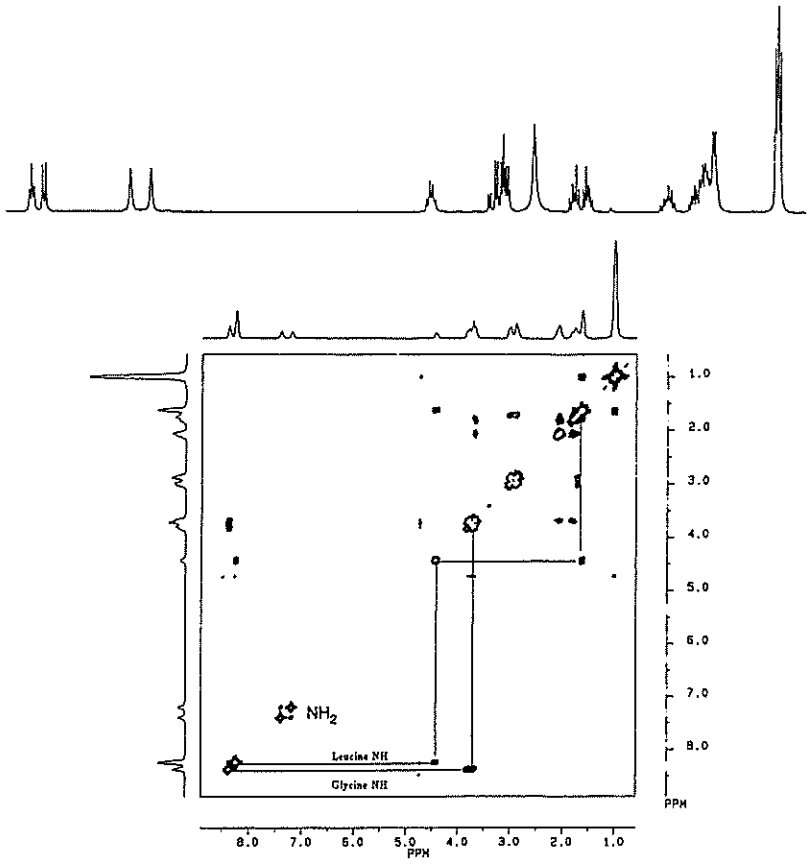

Figure 6-9 (Top) The 300 MHz ^1H spectrum of the tripeptide Pro-Leu-Gly in DMSO. (Bottom) COSY spectrum of Pro-Leu-Gly with connectivities of the NH protons. (Courtesy of IBM Instruments, Inc.)

connectivities, so the molecule consists of four independent spin systems: proline, leucine, glycine, and the terminal amide. The 1D ^1H spectrum is given at the top of Figure 6-9 without assignment. The high frequency (low field) peaks (δ 7.0–8.3) are from the protons on nitrogen, and the broad peak at δ 3.3 is from HOD. Figure 6-9 at the bottom contains the COSY spectrum with connectivities drawn in for the amide resonances. The nonequivalent terminal NH_2 resonances are immediately assigned as δ 7.0 and 7.2 because they have no external connectivities and hence no cross peaks other than between themselves. The Gly NH proton is assigned at δ 8.2 because it is a triplet (next to a CH_2) and has only the single connectivity with the CH_2 group at δ 3.6 (completing the Gly portion of the molecule). The remaining NH resonance at δ 8.1 is from Leu. It is a doublet (next to a CH) and has a cross peak with the resonance at δ 4.3, which has other connectivities. There is no third NH resonance, so the Pro NH must be quadrupolar-broadened or exchanging with HOD.

The upper portion of Figure 6-10 completes the COSY analysis of the Leu portion and confirms that the NH at δ 8.1 is part of Leu rather than Pro. The expected Leu connectivity is NH⟶ CH⟶ CH_2⟶ CH⟶ CH_3. Cross peaks with the following connectivities are observed (starting with NH): δ 8.1⟶ 4.3(q or dd)⟶ 1.5 (m)⟶ 0.9(dd). Apparently two of the proton resonances coincide, mostly likely those from CH_2 and the isopropyl CH. The CH_3 resonance as expected is at the lowest frequency and cannot be from any Pro group. Its higher multiplicity (dd, Figure 6-9, top) arises because the two methyl groups are diastereotopic due to the chiral center to which the butyl group is attached.

The lower portion of Figure 6-10 provides the Pro connectivity. The highest frequency resonance (δ 3.7) should be from the CH group adjacent (α) to the carbonyl group. The resonance at δ 3.7 actually is an overlap of this Pro CH (higher frequency

portion) and the Gly CH_2 (lower frequency portion). The Pro CH has two cross peaks with the diastereotopic β protons at δ 1.7 and 1.9, which are mutually coupled and have their own cross peak. Unfortunately, the γ protons are nearby (δ 1.6), but their cross peak with the δ protons at δ 2.8 completes the assignment of the spectrum. The fully assigned 1D spectrum and structure are given in Figure 6-11.

False peaks and lack of symmetry around the diagonal are common in the COSY experiment and can arise for several reasons. (1) Differences in digital resolution in the two time periods, t_1 and t_2, prevent perfect symmetry. (2) Incorrect pulse lengths or (3) incomplete transverse relaxation during the delay time can create false cross peaks. (4) We ignored the possibility of longitudinal relaxation. Magnetization in the z direction does not precess and therefore is rotated by the second 90° pulse into the position rec-

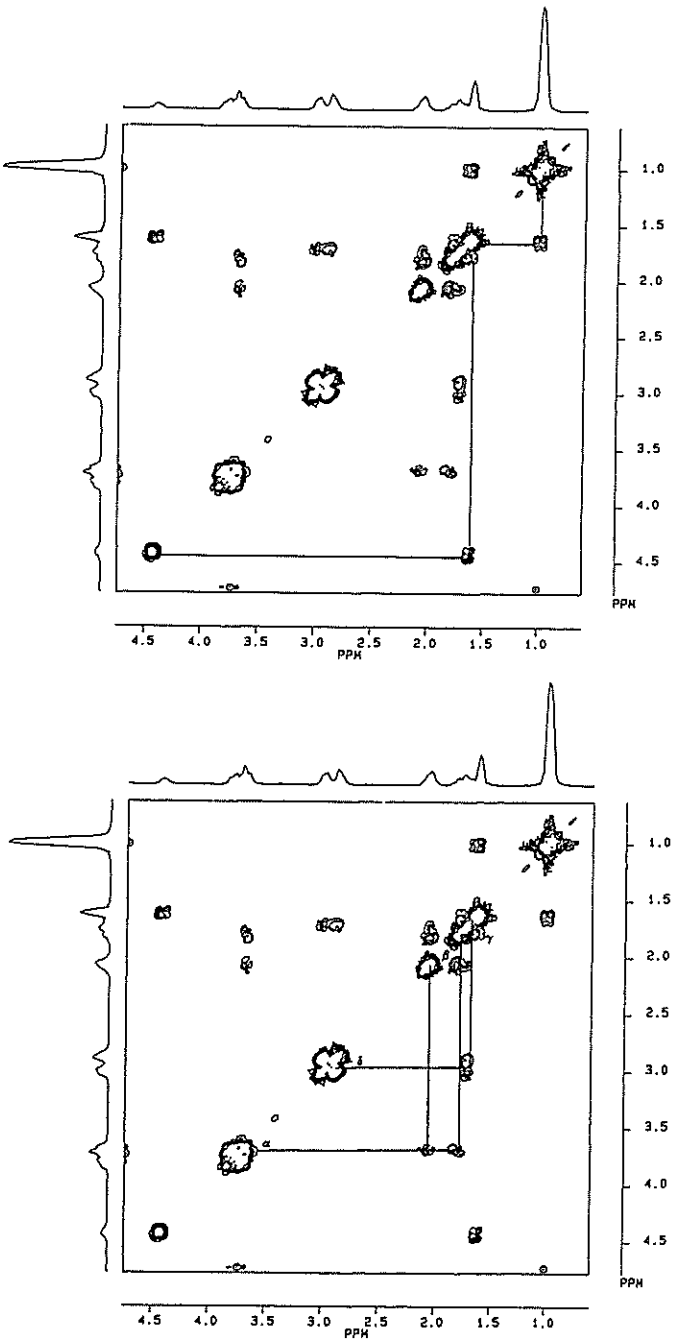

Figure 6-10 (Top) Connectivity within the leucine portion of Pro-Leu-Gly by COSY. (Bottom) Connectivity within the proline portion of Pro-Leu-Gly by COSY. (Courtesy of IBM Instruments, Inc.)

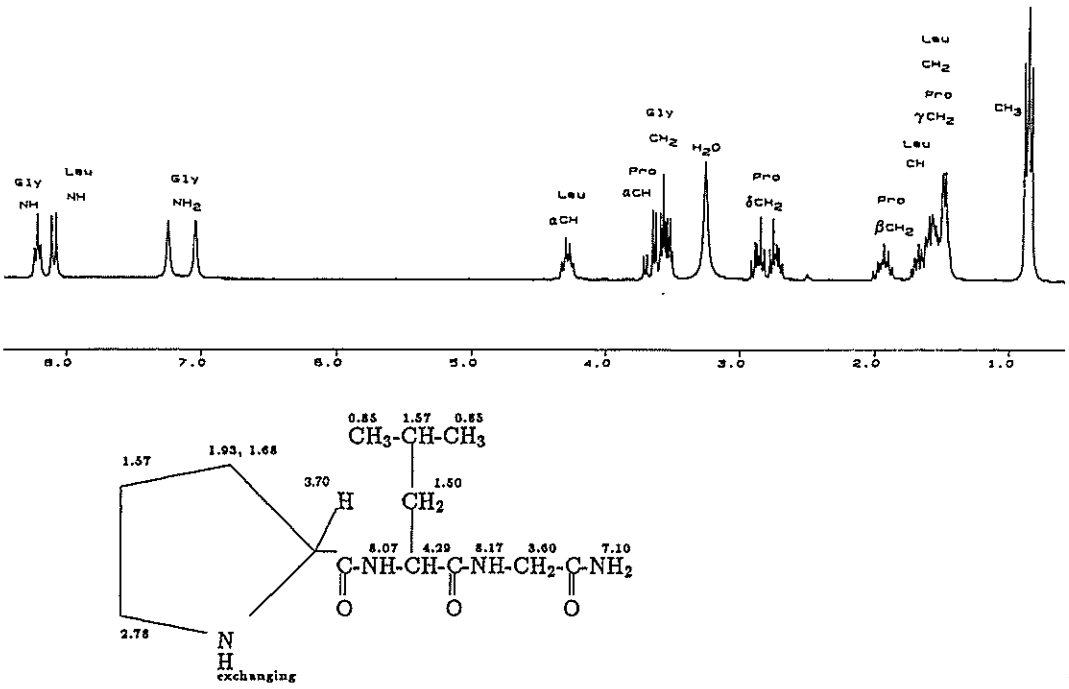

Figure 6-11 The fully assigned ^1H spectrum of Pro-Leu-Gly. (Courtesy of IBM Instruments, Inc.)

ognized as $v = 0$ (the position of the reference frequency). A stream of lines, called axial peaks, can occur at this frequency in the 2D plot. (5) Folding can occur in two dimensions and can give rise to off-position diagonal peaks and even cross peaks. All these artifacts may be minimized by optimizing pulse lengths, allowing sufficient time for transverse relaxation, use of phase cycling, and symmetrization. Axial peaks may be suppressed largely by alternating $+90°$ and $-90°$ for the second pulse, thus canceling z magnetization. The more complex CYCLOPS procedure provides suppression of axial peaks as well as elimination of other artifacts such as quad images (see Section 5-8). *Symmetrization* is a procedure for imposing bilateral symmetry around the diagonal. Most artifacts are conveniently eliminated by this procedure, but not all. For example, if two resonances have streams of axial lines, a point on one stream can occur at the precise mirror position (with respect to the diagonal) of a point on the other stream. Although the streams are largely eliminated, the two peaks at the symmetrical positions are retained and appear as handsome cross peaks. Usually common sense can reject them.

There are many variants of the standard COSY experiment that either improve on its basic aims or provide new information. We shall consider several of them without appreciable attention to the details of the pulse sequences.

COSY45. The large size of diagonal peaks sometimes can be a deterrent to understanding the significance of nearby cross peaks. The problem is aggravated by the presence of cross peaks from parallel transitions (see above). The COSY45 experiment reduces the intensities of the diagonal peaks and the cross peaks from parallel transitions. Figure 6-12 compares the COSY90 and COSY45 experiments for 2,3-dibromopropionic acid ($CH_2BrCHBrCO_2H$). The COSY45 experiment clarifies cluttered regions close to the diagonal but also provides information on the signs of coupling constants. The name derives from alteration of the second pulse length: $90° - t_1 - 45° - t_2$.

Long-Range COSY (LRCOSY). The normal assumption in the COSY experiment is that two- or three-bond (geminal or vicinal) couplings provide the dominant magnetization transfer to create cross peaks. Information from longer range couplings, however, also can be useful. Introducing a fixed delay Δ during the evolution and detection periods ($90° - t_1 - \Delta - 90° - \Delta - t_2$) enhances magnetization transfer from small cou-

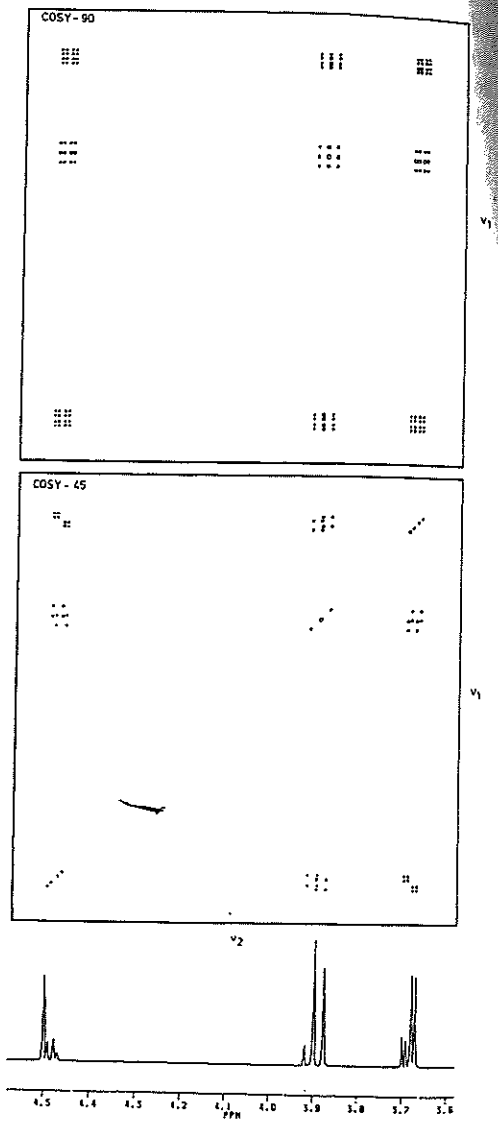

Figure 6-12 The COSY90 (top) and COSY45 (bottom) spectra of 2,3-dibromopropionic acid. The 1D spectrum at the bottom is a cross section through the COSY45 spectrum. (Reproduced from A.E. Derome, *Modern NMR Techniques for Chemistry Research,* Pergamon Press, Oxford, UK, 1987, p. 228.)

plings at the expense of large couplings. Figure 6-13 compares the COSY and LRCOSY experiments for a polynuclear aromatic compound. In the COSY spectrum, cross peaks occur only between ortho neighbors (a-b and e-f). In the LRCOSY spectrum, additional cross peaks arise between peri neighbors (c-d and d-e). Information on the connectivity between fused aromatic rings thus becomes available in the LRCOSY case.

Phase-Sensitive COSY. Fourier transformation involves building up the signal from the sum of sine and cosine curves. Every point in the spectrum has both sine and cosine contributions, which are 90° out of phase. These contributions sometimes are called the imaginary and real terms and lead mathematically to the *dispersion mode* and *absorption mode* spectra. An in-phase or absorption signal has the familiar form of a positive peak. The dispersion signal, commonly used for electron spin resonance spectra, has a sideways S shape with a portion below and a portion above the baseline. It produces both negative and positive maxima for a given peak and a value of zero at the resonance frequency as the sign changes. NMR experiments normally are tuned to the absorption mode by the process of phasing, but the two signals also may be combined mathematically to produce what is called a *magnitude spectrum.*

Many of the COSY experiments displayed so far used magnitude representations because of phase differences between various peaks in the pure modes. Magnetization that is not transferred (and thus appears on the diagonal) and magnetization that is transferred to parallel transitions undergo no phase shift. Cross peaks

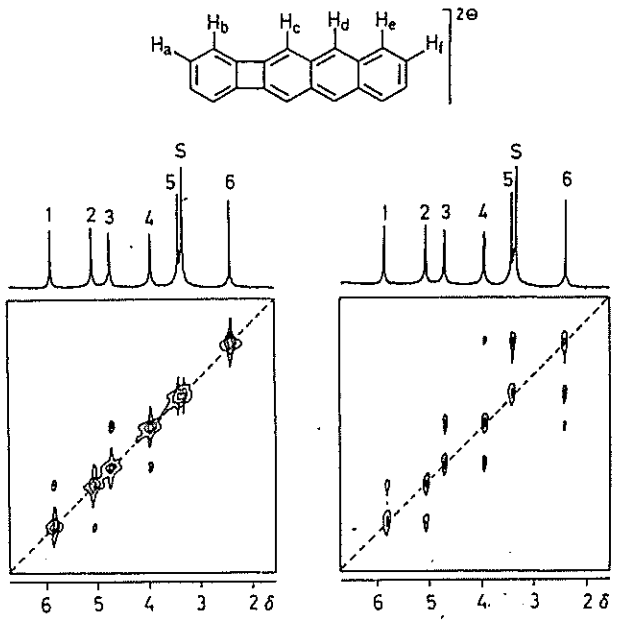

Figure 6-13 The 400 MHz COSY (left) and LRCOSY (right) spectra of naphthobiphenylene dianion (the signal S is from solvent). (Reproduced from H. Günther, *NMR Spectroscopy,* 2nd ed., John Wiley & Sons, Ltd., Chichester, UK, 1995, p. 300.)

rience phase shifts. Transfer between progressive transitions (A1 to X2 in Figure 6-5) shifts the phase −90°, and transfer between regressive transitions (A1 to X1) shifts it +90°. Because absorption and dispersion modes differ by 90°, phasing the diagonal peak to absorption results in dispersive cross peaks, or vice versa. Moreover, cross peaks from progressive and regressive transitions are always out of phase by 180° (if one is positive absorption, the other is negative absorption; or if one begins a dispersive signal negatively, the other begins positively). The magnitude or absolute value mode is used to eliminate all phase differences and produce absorption-like peaks. The resulting peaks tend to be broad and often are distorted. In small molecules with little peak overlap, there may be no problem with the use of magnitude spectra, but larger molecules such as proteins, polysaccharides, or polynucleotides may produce unacceptable overlap. Use of the phase-sensitive COSY experiment then can tune the cross peaks to a purely absorption (real) mode. This experiment not only provides enhanced resolution but also enables coupling constants to be read more easily from the cross peaks.

Because the 2D method involves two time domains, transformation in both t_1 and t_2 generates real and imaginary components. As a result, the phase-sensitive 2D signal has four modes rather than two. These phase modes or quadrants correspond to both frequency signals being real, both being imaginary, or one being real while the other is imaginary. Figure 6-14 illustrates the four modes. The real/real (RR) mode produces the familiar peak with a contour shaped like a four-pointed star at the base. Figure 6-15 illustrates what the COSY spectrum for two spins looks like when the diagonal and parallel components are tuned dispersively (both imaginary) and the progressive and regressive cross peaks are tuned absorptively (both RR but 180° out of phase). This common phase sensitive representation provides straightforward identification of the cross peaks derived from coupling and hence the determination of J.

Multiple Quantum Filtration. The one-dimensional INADEQUATE pulse sequence suppresses the centerband singlet in order to measure ^{13}C–^{13}C couplings from the satellites (see Section 5-7). The procedure involves creating double quantum coherences. A similar procedure may be used in two dimensions to suppress singlets, which are single quantum coherences. Such singlets may arise from solvent or from uncoupled methyl resonances, both of which can constitute major impediments in locating highly

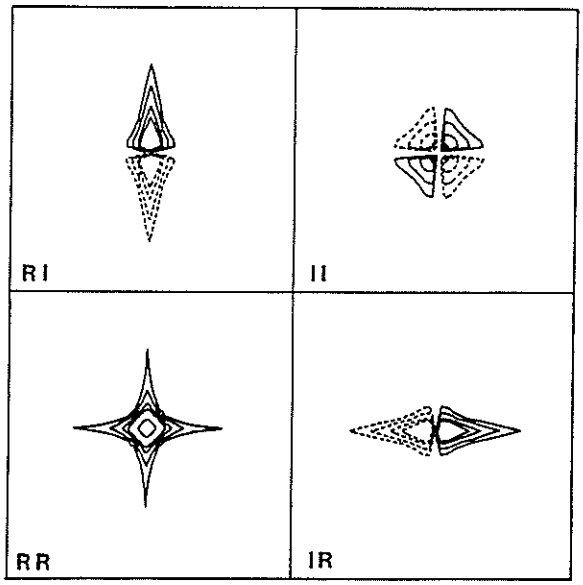

Figure 6-14 The four types of 2D phase quadrants, corresponding to frequency modes that are real/real (RR), imaginary/real (IR), real/imaginary (RI), and imaginary/imaginary (II). (Reproduced from A.E. Derome, *Modern NMR Techniques for Chemistry Research*, Pergamon Press, Oxford, UK, 1987, p. 207.)

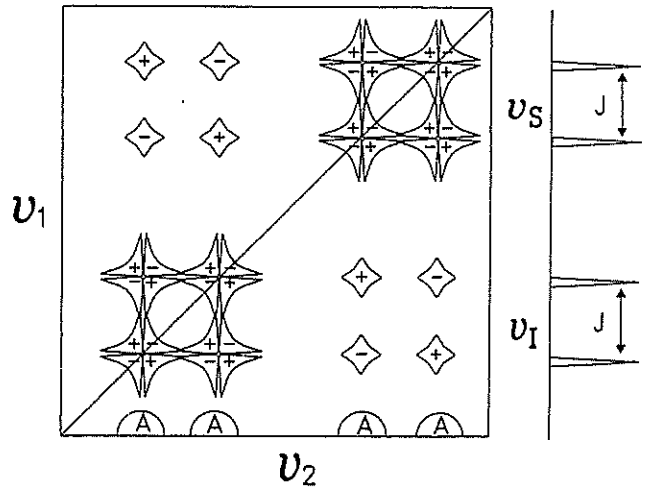

Figure 6-15 Phase-sensitive COSY diagram for two spins, with the diagonal peaks in dispersion mode and the cross peaks in antiphase absorption mode. The 1D spectrum is on the right. (Reproduced from F.J.M. van de Ven, *Multidimensional NMR in Liquids*, VCH, New York, 1995, p. 171.)

split resonances in a complex spectrum. In a double quantum filtered COSY (DQF–COSY) experiment, an extra 90° pulse is added after the second 90° COSY pulse, and phase cycling converts multiple quantum coherences into observable magnetizations. The resulting 2D spectrum lacks all singlets along the diagonal (for example, the left spectrum in Figure 6-16). An important feature of the phase-sensitive DQF–COSY experiment is that double quantum filtration allows both diagonal and cross peaks to be tuned into pure absorption at the same time. This feature reduces the size of all the diagonal signals and permits analysis of cross peaks close to the diagonal. The only disadvantage of DQF–COSY is reduction in sensitivity by a factor of two. The triple quantum filtered COSY experiment (TQF–COSY) removes both singlets and AB or AX quartets, provid-

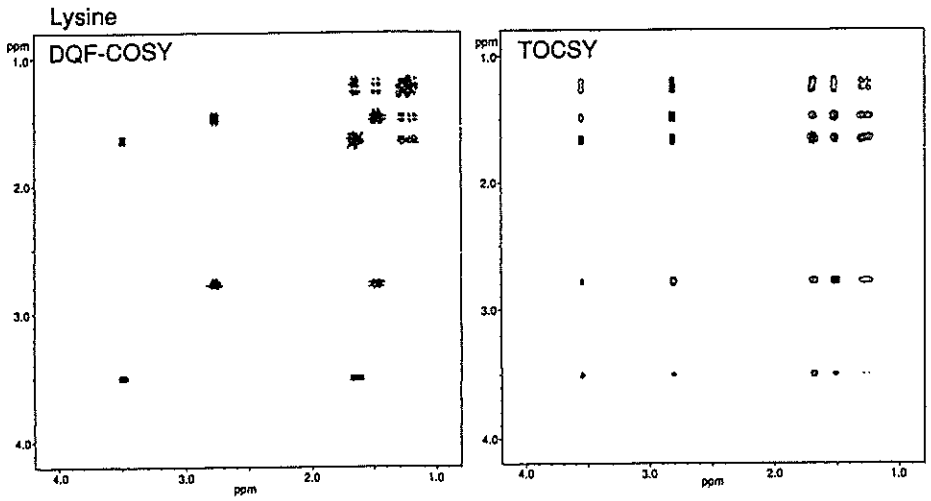

Figure 6-16 The DQF–COSY and TOCSY spectra of lysine. (Reproduced from J.N.S. Evans, *Biomolecular NMR Spectroscopy*, Oxford University Press, Oxford, UK, 1995, p. 428.)

Total Correlation Spectroscopy (TOCSY). The connectivity within an entire spin system such as in a butyl group ($CH_3CH_2CH_2CH_2$—), must be mapped out in the standard COSY experiment from proton to proton via a series of cross peaks. By spin locking the protons during the second COSY pulse, the chemical shifts of all the protons may be brought essentially into equivalence. Recall that resonance frequencies of protons and carbons are made equal through cross polarization for solids by achieving the Hartmann-Hahn condition (see Section 2-10). In the 2D variant of this experiment, the initial 90° pulse and the t_1 period occur as usual, but the second pulse locks the magnetization along the y axis so that all protons have the spin lock frequency. All coupled spins within a spin system then become closely coupled and magnetization is transferred from one spin to all other members. Figure 6-16 on the right shows the result for lysine [$NH_2CH(CH_2\ CH_2CH_2CH_2NH_2)CO_2H$]. The methylene group at the lowest frequency (upper right corner) exhibits four TOCSY cross peaks, one with each of the other three methylene protons and one with the methine proton. The TOCSY experiment, a variation of which is called the **HO**monuclear **HA**rtmann-**HA**hn or HOHAHA experiment, has particular advantages for large molecules. It has enhanced sensitivity, and both diagonal and cross peaks may be phased to the absorption mode. The process of identifying resonances within specific amino acid or nucleotide residues is considerably simplified by this procedure. Each residue can be expected to exhibit cross peaks among all its protons and none with protons of other residues.

Relayed COSY. An alternative but less general method for displaying extended levels of connectivity is provided by relayed coherence transfer (RCT). The normal COSY experiment for an AMX system with $J_{AX} = 0$ produces cross peaks between A and M and between M and X. It is not unusual for the key diagonal peak for M to be coincident with a resonance from another spin system, making it difficult to follow the connectivity path (for example, recall the Leu portion of the COSY spectrum of Pro-Leu-Gly in Figure 6-10). The RCT experiment generates a cross peak between the A/M and M/X cross peaks, eliminating the ambiguity. The RCT pulse sequence is $90°–t_1–90°–\tau–180°–\tau–90°–t_2$, in which the sequence after the second 90° pulse permits relay of coherence to the next spin. The result is shown diagrammatically in Figure 6-17 for AMX and A'M'X' systems whose M and M' resonances coincide. The COSY experiment contains the expected four cross peaks. The RCT experiment additionally contains two cross peaks connecting the cross peaks of the individual spin systems, labeled (A,M,X) and (A',M',X'). The connectivity of A⟶M⟶X and of A'⟶M'⟶X' is then rendered unambiguous.

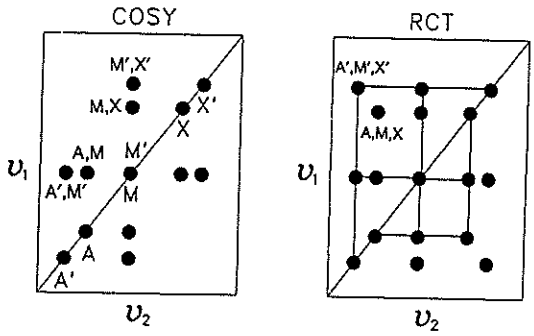

Figure 6-17 Diagram of COSY and relayed coherence transfer (RCT) experiments for two three-spin systems (AMX and A'M'X') whose M and M' portions overlap. (Adapted from F.J.M. van de Ven, *Multidimensional NMR in Liquids*, VCH, New York, 1995, p. 233.)

J-Resolved Spectroscopy. In Chapter 5 we saw how the spin echo experiment can isolate or remove characteristics of chemical shifts or coupling constants. Spin echoes may be used in two dimensions to generate one frequency dimension representing chemical shifts and another coupling constants. The sequence $90° - \frac{1}{2}t_1 - 180° - \frac{1}{2}t_1 - t_2$ for example uses the 180° pulse to refocus chemical shifts during t_1. The result for a glucose derivative is shown in Figure 6-18. The ^1H frequencies are found on the horizontal axis (ν_2), with the normal 1D spectrum displayed at the top (a). The vertical axis ("f_1" = ν_1) contains only proton–proton coupled multiplets, each centered about a zero frequency point, that is, all multiplets occur at the same chemical shift in ν_1. Thus the multiplet at highest frequency (lowest field) from H-3 is a quartet with further splitting when viewed from the vertical axis. By taking a projection at an angle (45°) that causes each of the members of the individual multiplets to overlap when viewed from the horizontal axis, as at the bottom (b), a display is obtained that in essence is a proton-proton decoupled proton spectrum. Resonances are present at each frequency devoid of any couplings. This projection is a novel way to examine ^1H spectra, although it has not seen widespread use because it reveals no connectivities.

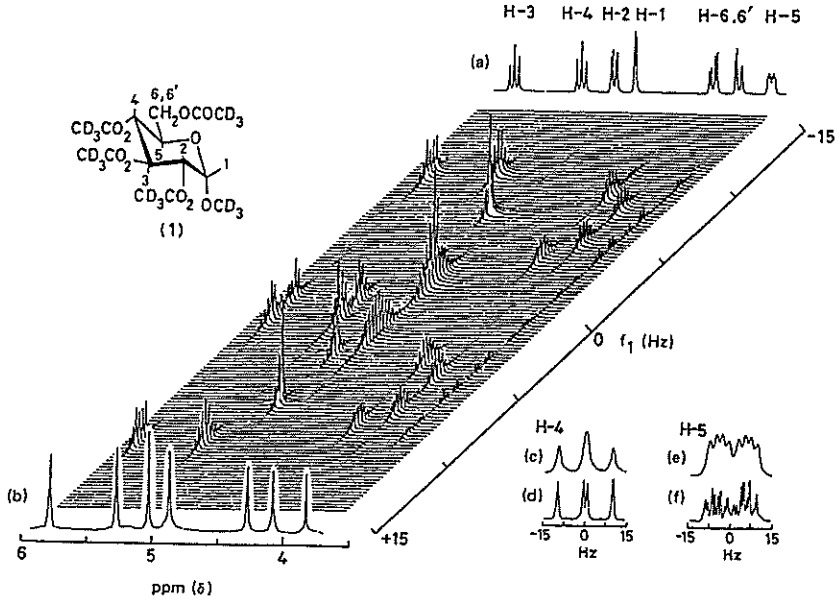

Figure 6-18 The 270 MHz 2D *J*-resolved ^1H spectrum of 2,3,4,6-tetrakis-*O*-trideuteroacetyl-α-D-glucopyranoside. (Reproduced from L.D. Hall, S. Sukumar, and G.R. Sullivan, *J. Chem. Soc., Chem. Commun.* 292 [1979].)

The pulse sequence, as a variant of the spin echo experiment, also refocuses the spread of frequencies caused by field inhomogeneity, so that some improvement in resolution is obtained. The inset at the lower right of Figure 6-18 shows the normal 1D spectra of H-4 and H-5 at the top (c and e) and the unrotated projection of the 2D *J*-resolved spectra at the bottom (d and f, extracted from the projected spectrum (a) at the top of the 2D display). The much higher resolution of the 2D resonances is clearly evident. Thus the procedure is an effective way to measure *J* accurately, particularly when *J* is poorly resolved in the 1D spectrum. The experiment fails for closely coupled nuclei (second order spectra).

In addition to resolving small couplings that may be absent in the 1D spectrum, the *J*-resolved procedure can be used to distinguish homonuclear from heteronuclear couplings. The vertical axis in Figure 6-18 displays couplings only between spins that experienced the 180° pulse. Thus only $^{1}H-^{1}H$ couplings appear on this axis. Couplings to heteronuclei are not phase modulated and consequently appear as spacings along the horizontal axis. In this way, $^{1}H-^{19}F$ and $^{1}H-^{31}P$ couplings may be distinguished from $^{1}H-^{1}H$ couplings, which are removed in the rotated spectrum such as that shown in (b) at the bottom of Figure 6-18.

6-2 PROTON–HETERONUCLEUS CORRELATION

Cross peaks in the COSY experiment are generated through magnetization transfer that arises from scalar *(J)* coupling between protons or between any identical nuclides. Coupling from a proton to a different nuclide such as carbon-13 should be able to generate a similar response. Analogous cross peaks then would provide very useful information about which carbons are bonded to which protons. Thus assignment of a proton resonance would automatically lead to the assignment of the resonance of the carbon to which it is bonded, and vice versa. The simplest extension of the COSY sequence to include magnetization transfer to carbon takes the form given in Figure 6-19. The pulse sequence is very reminiscent of the one-dimensional INEPT sequence, and manipulation of magnetization is much the same (see Figure 5-19). The initial 90° ^{1}H pulse generates *y* magnetization. For the simplest case of one carbon bonded to one proton (as in $CHCl_3$), ^{1}H magnetization evolves during the period t_1 according to its Larmor frequency. Two ^{1}H vectors diverge due to coupling with ^{13}C. The second 90° ^{1}H pulse generates nonequilibrium *z* magnetization that is transferred to ^{13}C as shown in Figure 5-19. The single 90° ^{13}C pulse then provides the ^{13}C free induction decay that is acquired during t_2. The 2D spectrum then has one axis in ^{1}H frequencies (ν_1) and one in ^{13}C frequencies (ν_2).

For the simple AX example the 2D spectrum contains two peaks when projected onto either the ^{1}H or the ^{13}C axis (the A and X portions of the AX spectrum). Thus the ^{1}H resonances that are detected actually are the ^{13}C satellites of the usual ^{1}H spectrum. The 2D display contains four peaks: two along a diagonal and two symmetrically off the diagonal. Moreover, the peaks are in antiphase for each nuclide, since the INEPT spectrum without decoupling generates one peak up and one peak down. Application of decoupling would result in algebraic summing of the peaks to zero.

To bring about decoupling, an additional pulse and two fixed time periods are added (Figure 6-20). The first ^{1}H pulse allows chemical shifts and coupling constants to evolve during t_1. The 180° ^{13}C pulse refocuses H–C coupling constants in the ^{1}H dimension (^{1}H is then decoupled from ^{13}C). The fixed time Δ_1 allows the ^{1}H vectors to obtain

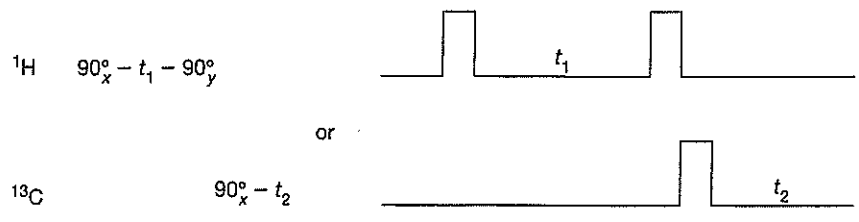

Figure 6-19

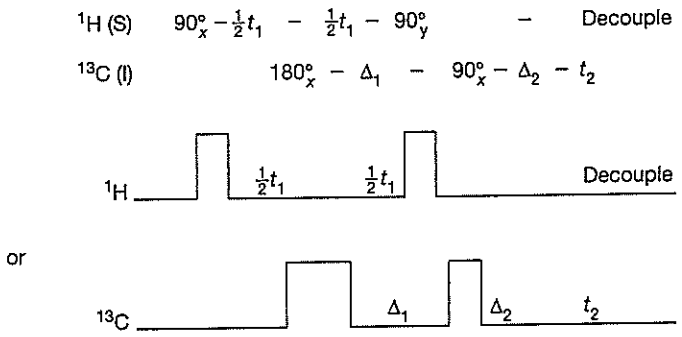

Figure 6-20

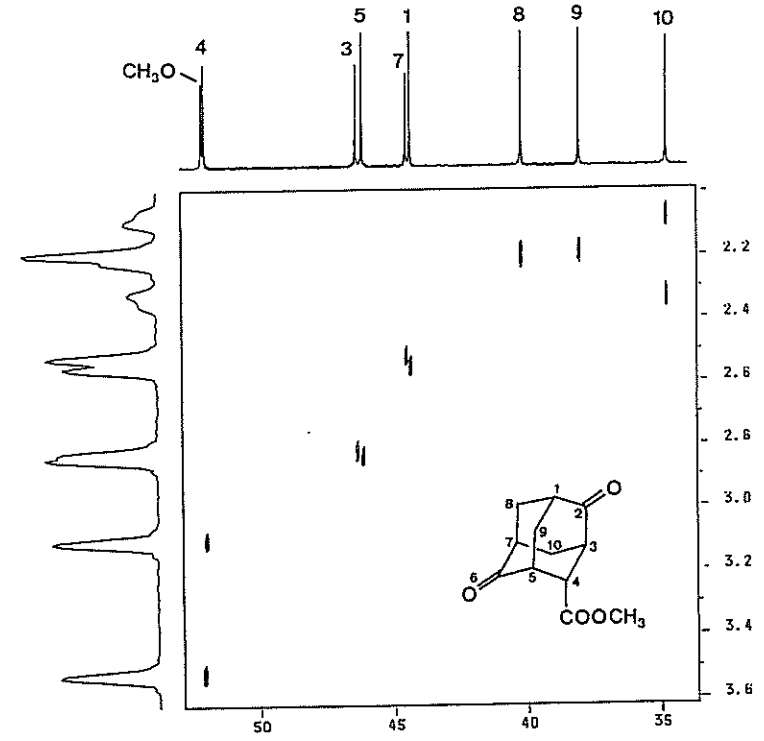

Figure 6-21 The HETCOR spectrum of 4-(methoxycarbonyl)adamantane-2,6-dione. (Reproduced from H. Duddeck and W. Dietrich, *Structure Elucidation by Modern NMR*, Steinkopff Verlag, Darmstadt, Germany, 1989, p. 22.)

the antiphase (180° out of phase) relationship illustrated in Figure 5-15. The second 90° ^{1}H pulse moves the vectors in antiphase relationship onto the z axis and provides polarization transfer to ^{13}C, also in antiphase relationship. The 90° ^{13}C pulse is for observation. The second fixed time Δ_2 restores phase alignment and permits ^{13}C to be decoupled from ^{1}H during ^{13}C acquisition.

Figure 6-21 illustrates this procedure for an adamantane derivative. The ^{1}H frequencies are on the vertical axis and the ^{13}C frequencies are on the horizontal axis. The respective spectra are illustrated on the left and at the top. The 2D spectrum is composed only of cross peaks, each one relating a carbon to its directly bonded proton(s). Quaternary carbons are invisible to the technique, as the fixed times Δ_1 and Δ_2 normally are set to values for one bond couplings. This experiment often is a necessary component in the complete assignment of ^{1}H and ^{13}C resonances. Its name, **HET**eronuclear chemical shift **COR**relation, usually is abbreviated as HETCOR, but other acronyms, HSC (**H**eteronuclear **S**hift **C**orrelation) and H,C COSY, also are used. The method may

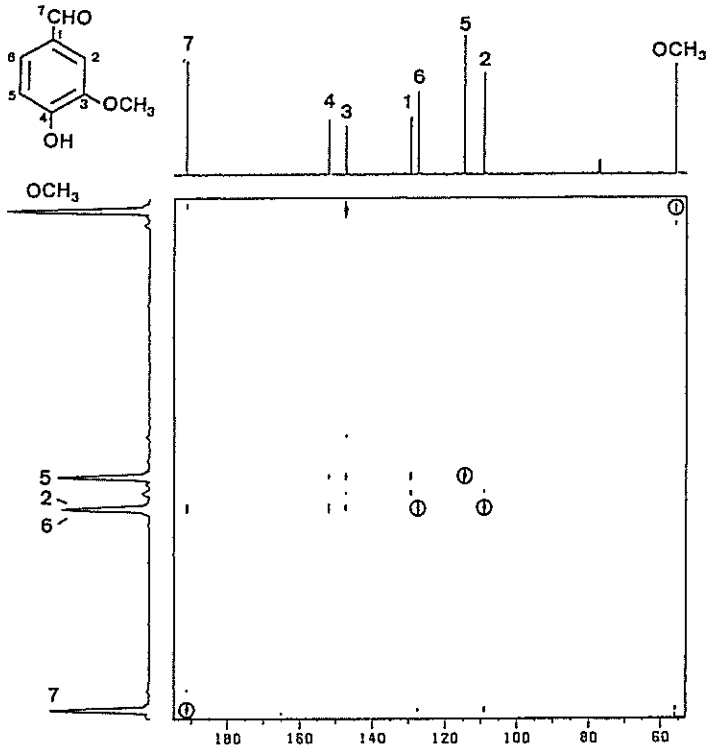

Figure 6-22 The COLOC spectrum of vanillin. (Reproduced from H. Duddeck and W. Dietrich, *Structure Elucidation by Modern NMR,* Steinkopff Verlag, Darmstadt, Germany, 1989, p. 24.)

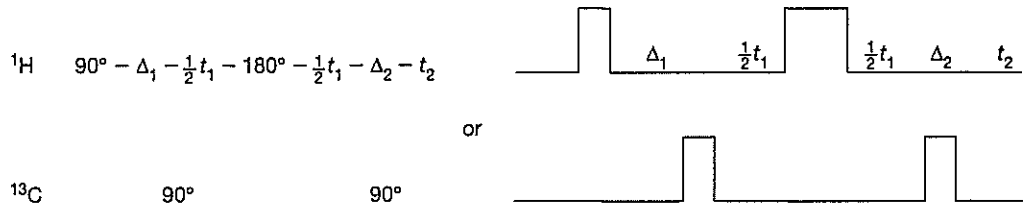

Figure 6-23

To focus on longer range H–C couplings, the fixed times Δ_1 and Δ_2 are lengthened accordingly. Loss of magnetization due to transverse relaxation then reduces sensitivity significantly. The COLOC pulse sequence (**CO**rrelation spectroscopy via **LO**ng-range **C**oupling) avoids this problem by incorporating the ^1H evolution period t_1 inside the Δ_1 delay period. Figure 6-22 shows a COLOC spectrum for vanillin. The circled cross peaks are residues from one bond couplings. The only long-range coupling of the methoxy group is with C-3, which indicates that methoxy is connected at that point. Other long range couplings are seen, for example, between C-1 and H-5, C-3 and H-5, and C-2 and H-7.

A major drawback to the HETCOR experiment is the low sensitivity that results from detection of the X nucleus (usually ^{13}C). The HMQC experiment (**H**eteronuclear correlation through **M**ultiple **Q**uantum **C**oherence) uses inverse detection, whereby ^{13}C responses are observed in the ^1H spectrum. The pulse sequence is given in Figure 6-23 and represents coherence rather than polarization transfer. The sequence is initiated by the 90° ^1H pulse, which creates ^{13}C polarization through the ^1H–^{13}C coupling constant during the fixed Δ_1 period. The remainder of the sequence is designed to select double quantum coherence (the ^{13}C satellites in the ^1H spectrum) over single quantum coherence (the ^1H centerbands), in a process similar to the 1D INADEQUATE experiment in Section 5-7. The 2D representation, as in Figure 6-24 for camphor, normally still includes the ^1H–^{13}C coupling information in the ^1H dimension, although ^{13}C irradiation can be carried out during the ^1H t_2 acquisition period.

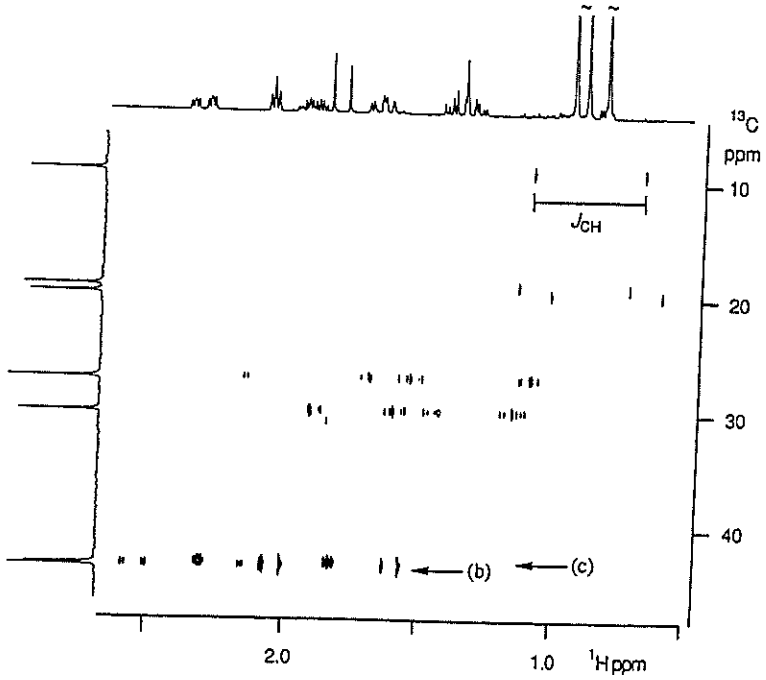

Figure 6-24 The HMQC spectrum of camphor, with $^{1}H-^{13}C$ couplings retained in the ^{1}H dimension. (Reproduced from J.K.M. Sanders and B.K. Hunter, *Modern NMR Spectroscopy,* Oxford University Press, Oxford, UK, 1993, p. 111.)

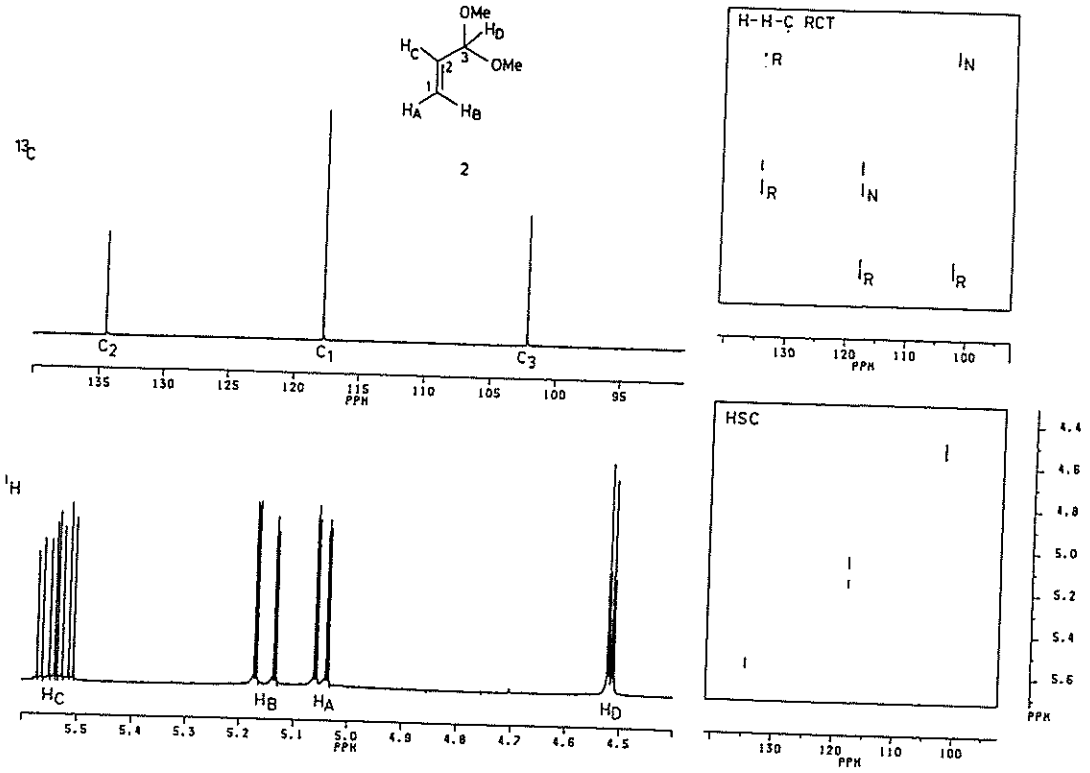

Figure 6-25 (Left) The ^{13}C and ^{1}H spectra of the dimethyl acetal of acrolein. (Right) The normal HETCOR (called HSC, bottom) and the H–H–C relay coherence transfer (top) experiments for the same molecule. (Reproduced from A.E. Derome, *Modern NMR Techniques for Chemistry Research,* Pergamon Press, Oxford, UK, 1987, p. 111.)

The relay experiment (RCT) may be adapted to the HETCOR context. The result of such an experiment is given in Figure 6-25. The normal HETCOR experiment ("HSC" in the figure) for the illustrated acetal of acrolein is given at the bottom right. The following cross peaks are present: (H_C/C-2) at the bottom left, (H_B/C-1) and H_A/C-1) in the middle, and (H_D/C-3) at the upper right. This experiment shows that C-3 is bonded to H_D, C-2 to H_C, and C-1 to H_A and H_B. The H–H–C relay coherence transfer experiment is shown at the upper right. The normal HETCOR cross peaks are labeled N, and that for H_C/C-2 is missing. The additional cross peaks result from relayed connectivity between given CH pieces. Thus the relayed (R) peak at the upper left indicates that H_D/C-3 and H_C/C-2 are connected. The relayed peak at the bottom left indicates connectivity between $H_{A/B}$/C-1 and H_C/C-2. The other two peaks labeled R are mirror images of these relayed peaks. This particular experiment is called H–H–C RCT because the pulses involve ^{1}H signals twice and ^{13}C signals once, in that order. Other heteronuclear relay experiments can involve a different order (H–C–H) or different nuclei (H–H–N).

6-3 PROTON–PROTON CORRELATION THROUGH SPACE OR CHEMICAL EXCHANGE

In the original depiction of the two-dimensional experiment in Figure 6-2, the magnetization vector was resolved into sine and cosine components during t_1. The sine component was followed through the second 90° pulse and into the t_2 domain to create the COSY sequence. We ignored the cosine component, which remained along the z axis after the second 90° pulse and hence was unobservable. There are mechanisms of magnetization transfer other than scalar coupling, and these can affect z magnetization and hence the cosine component. Irradiation at the frequency of one proton can transfer magnetization to nearby protons through dipolar interactions (the nuclear Overhauser effect). Its clear effect on z magnetization is reflected in spectral intensity perturbations in one dimension (see Section 5-4). In addition, alteration of the chemical identity of a nucleus through chemical exchange affects z magnetization. A nucleus resonating at one frequency turns into another nucleus resonating at a different frequency but carrying its population information to the new site (see Section 5-2).

With reference to Figure 6-2d, that is, after the second 90° pulse, both the NOE and the chemical exchange mechanisms can modulate the cosine component of the magnetization along the z axis. The frequency of modulation is the frequency of the magnetization transfer partner, either from dipolar relaxation or chemical exchange. After a suitable, fixed period of time, during which this modulation is optimized (τ_m, the mixing period), the cosine component may be moved to the xy plane by a third 90° pulse and detected along the y axis during a t_2 acquisition period. Thus the complete experiment is $90°-t_1-90°-\tau_m-90°-t_2$. Because the frequency of magnetization during t_1 moves to another value during τ_m and is observed at the new frequency during t_2, the two-dimensional representation of this experiment exhibits cross peaks. When the cross peaks derive from magnetization transfer through dipolar relaxation, the 2D experiment is called NOESY (**NOE S**pectroscop**Y**). When they derive from chemical exchange, it is called EXSY (**EX**change **S**pectroscop**Y**).

The duration of the fixed time τ_m depends on the relaxation time T_1, the rate of chemical exchange, and the rate of NOE buildup. In the case of the NOESY experiment, valuable information is provided about the distance between various protons within a molecule. Figure 6-26 illustrates the NOESY spectrum for a complex heterocycle. The 1D spectrum, as with COSY, is found along the diagonal, and off-diagonal or cross peaks occur when two protons are close in space. Thus methyl group **l** shows an expected cross peak with the adjacent alkenic proton **a** (upper left). Additional cross peaks of methyl **l** indicate closeness to the methinyl proton **f** and the acetal methyl **n.** The ester methyl **e** is close to the other acetal methyl **m.** The NOESY experiment thus can provide both structural and conformational information. In practice, cross peaks become unobservable when the proton–proton distance exceeds about 5 Å.

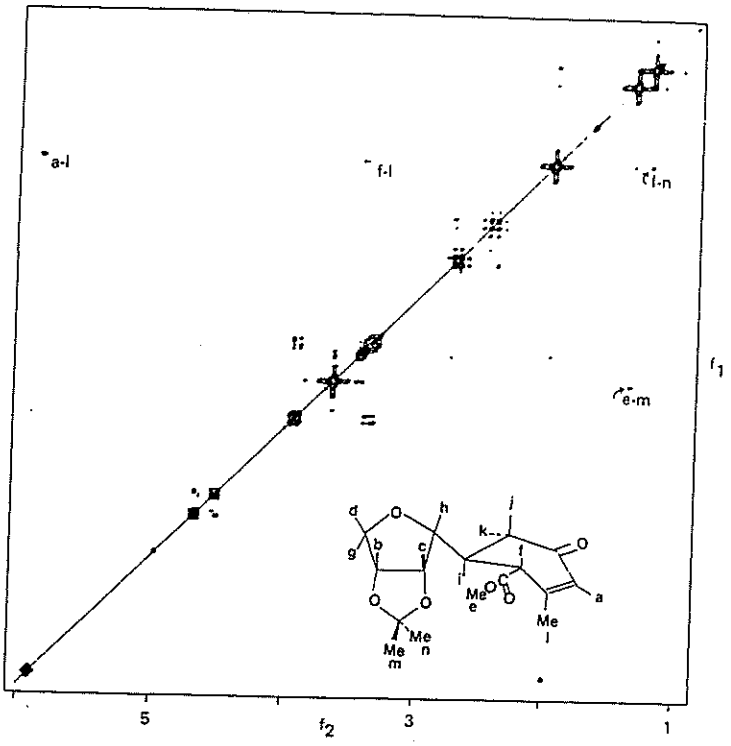

Figure 6-26 The ^{1}H NOESY spectrum for the indicated compound. (Courtesy of Bruker Instruments, Inc.)

At least three factors complicate the analysis of NOESY spectra. First, COSY signals may be present from scalar couplings and may confuse an analysis intended to be based entirely on interproton distances (vicinal couplings, for example, are largest when they are furthest apart, found in the antiperiplanar geometry). COSY signals may be eliminated through phase cycling or by a statistical variation of τ_m by about 20% (the NOESY signals grow monotonically but the COSY signals are sinusoidal).

Second, in small molecules the NOE tends to build up slowly and attain a theoretical maximum of only 50%, as noted earlier in the 1D context (see Section 5-4). Because a single proton may be relaxed by several neighboring protons, the actual maximum normally is much less than 50% (the same problem of course exists in the 1D NOE experiment). Moreover, as molecular size increases and behavior departs from the extreme narrowing limit, the maximum NOE decreases to zero and becomes negative. Thus for many small to medium-sized molecules the NOESY experiment may fail. For larger molecules, whose relaxation is dominated by the W_0 term, not only is the maximum NOE -100% rather than $+50\%$, but also the NOE buildup occurs more rapidly. The NOESY experiment thus has been of particular utility in the analysis of the structure and conformation of large molecules such as proteins and polynucleotides.

Third, in addition to direct transfer of magnetization from one proton to an adjacent proton, magnetization may be transferred by spin diffusion. In this mechanism, already described in the 1D experiment (see Section 5-4), magnetization is transferred through the NOE from one spin to a nearby second spin and then to a third spin. The third spin is close to the second spin but not necessarily to the first spin. These multistep transfers thus can produce NOESY cross peaks between protons that are not close together. Spin diffusion can even occur through two or more intermediate spins, but the process becomes increasingly less efficient. Direct magnetization transfer and transfer by spin diffusion sometimes may be distinguished by examination of the NOE buildup rate, as illustrated in Figure 6-27. In this hypothetical plot of the NOE intensity as a function of the fixed time τ_m for irradiation at the A frequency of a system D–A-B-C, AA is the intensity of the diagonal peak and

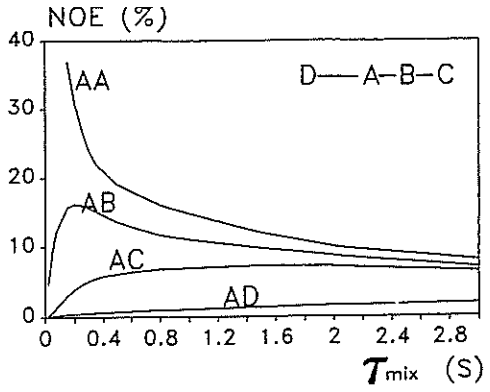

Figure 6-27 Peak intensities calculated for a hypothetical NOESY experiment involving four nuclei, D–A-B-C, with D 4 Å from B and B 2 Å from A and C. The curve labeled AA is for the diagonal peak, and the remaining curves are for the various cross peaks. (Reproduced from F.J.M. van de Ven, *Multidimensional NMR in Liquids,* VCH, New York, 1995, p. 188.)

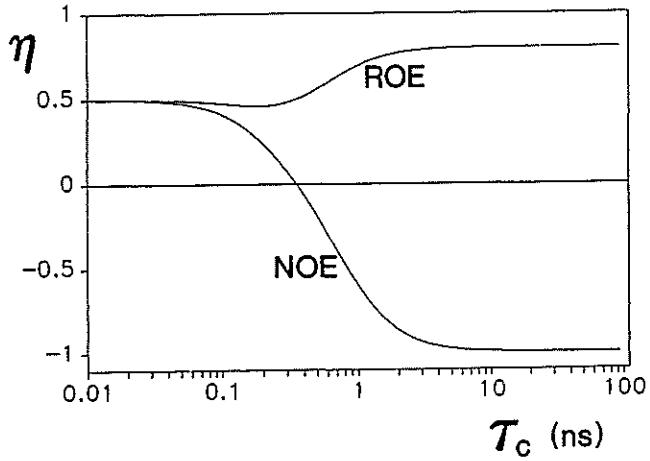

Figure 6-28 The enhancement factor η as a function of the effective correlation time τ_c for the standard nuclear Overhauser experiment (NOE) and for the spin lock or rotating coordinate variant (ROE). The curves were calculated for an interproton distance of 2.0 Å and a spectrometer frequency of 500 MHz. (Reproduced from F.J.M. van de Ven, *Multidimensional NMR in Liquids,* VCH, New York, 1995, p. 251.)

model) rises most rapidly. Protons A and D are 4 Å apart and show a very small NOE. Protons A and C also are 4 Å apart (2 Å between A and B and another 2 Å between B and C), but the intensity of the AC cross peak rises steadily through spin diffusion with B as the intermediary. The model shows that spin diffusion provides the major contribution to the AC cross peak for a distance of 4 Å, but the buildup is slower than for the direct transfer for the AB cross peak.

The rotating frame NOESY (ROESY) experiment provides some advantages for small and medium-sized, as well as large molecules. Whereas the NOE decreases to zero and becomes negative as the mean correlation time τ_c for molecular rotation increases (larger molecules move more slowly), in the rotating frame the maximum NOE remains positive and even increases from 50% to 67.5% (Figure 6-28). The pulse sequence for ROESY (previously called CAMELSPIN) is similar to TOCSY or HOHAHA, although the period of spin locking is chosen to optimize magnetization transfer through the NOE (dipolar interactions) rather than through scalar couplings. In addition to greater signal enhancement, the ROESY experiment also decreases spin diffusion, so that it offers advantages for large molecules. Just as COSY artifacts may be present in the NOESY spectrum, so can TOCSY artifacts be present in the ROESY spectrum, and steps must be taken to remove them. Use of a weak static spin-lock pulse can reduce the TOCSY peaks.

When magnetization is transferred via chemical exchange in the EXSY experiment, it may be necessary to perform several preliminary experiments to optimize the

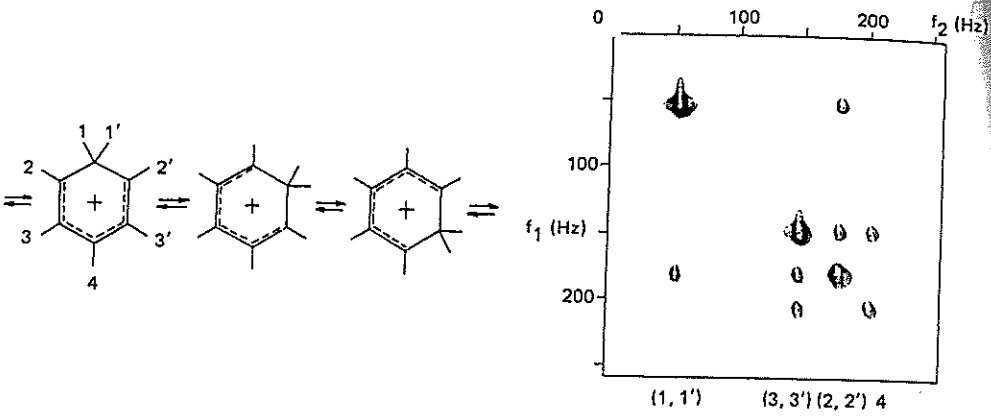

Figure 6-29 The ^{1}H EXSY spectrum for the heptamethylbenzenium ion. (Reproduced with permission from R.H. Meier and R.R. Ernst, *J. Am. Chem. Soc.*, **101**, 6441 [1979]). Copyright 1979 American Chemical Society.)

value of τ_m, which should be approximately $1/k$. Figure 6-29 contains the EXSY experiment from an early example by Ernst, in which the diagonal peaks run nontraditionally from upper left to lower right. At fast exchange the 1D ^{1}H spectrum of the heptamethylbenzenium ion contains only one methyl resonance, as the methyl group moves around the ring. At slow exchange there are distinct resonances for the four types of methyls labeled on the left in the figure. The EXSY experiment shows which methyls interchange with which. One can imagine 1,2, 1,3 or 1,4 shifts, but the EXSY experiment agrees only with the 1,2 mechanism. Each off-diagonal peak indicates magnetization transfer between two diagonal peaks. Thus the 1 methyls have a cross peak only with (and hence exchange only with) the 2 methyls; the 2 methyls exchange with the 1 and 3 methyls; the 3 methyls exchange with the 2 and 4 methyls; and the 4 methyls exchange only with the 3 methyls. This is the pattern expected for 1,2 shifts.

The intensity of the cross peaks depends on the rate constant for exchange. For the case of exchange between equally populated sites lacking spin–spin coupling (for example the two methyls of *N*,*N*-dimethylformamide, $H(CO)N(CH_3)_2$), the rate constant k is related to the mixing time τ_m, the intensity of the cross peak I_c, and the intensity of the diagonal peaks I_d by eqs. 6-1 and 6-2.

$$I_d/I_c \sim (1 - k\tau_m)/k\tau_m \tag{6-1}$$

$$k \sim 1/[\tau_m(I_d/I_c + 1) \tag{6-2}$$

6-4 CARBON–CARBON CORRELATION

The 1D INADEQUATE experiment provides a method for measuring ^{13}C–^{13}C coupling constants and for determining carbon–carbon connectivity by establishing coupling magnitudes that are common to two carbon atoms (see Section 5-7). In practice, application to solving connectivity problems is complicated not only by the inherently low sensitivity of detecting two dilute nuclei but also by the similarity of many ^{13}C–^{13}C couplings. Duddeck and Dietrich have pointed out that all the one-bond carbon–carbon couplings in cyclooctanol fall in the narrow region 34.2–34.5 Hz, except for C-1–C-2, which is 37.5 Hz. This latter problem may be largely alleviated by translating the experiment into two dimensions. The original INADEQUATE experiment (see Section 5-7) can be adapted directly to two dimensions by incrementing the fixed time Δ as the t_1 domain: $90^\circ_x - 1/4J_{CC} - 180^\circ_y - 1/4J_{CC} - 90^\circ_x - t_1 - 90^\circ_\phi - t_2$.

The time period t_1 is used to encode the double quantum frequency domain. The resulting 2D display contains a horizontal axis in ν_2 (the normal ^{13}C frequencies) and a vertical axis that is a double quantum domain represented by the sum of the frequencies of coupled ^{13}C nuclei ($\nu_1 = \nu_A + \nu_B$). The pattern of cross

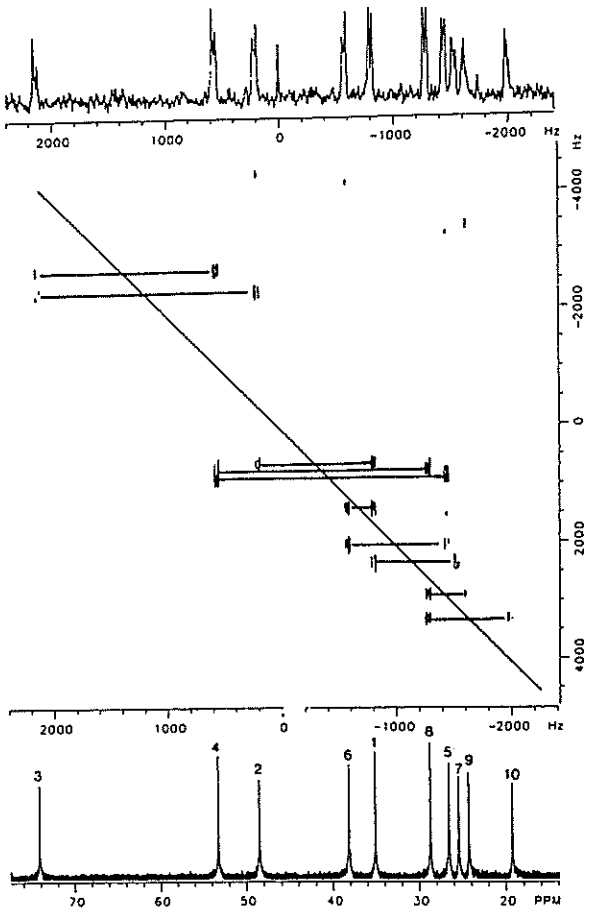

Figure 6-30 The 2D INADEQUATE spectrum of menthol, with the ^{1}H-decoupled ^{13}C spectrum at the bottom and the ^{13}C-coupled ^{13}C spectrum at the top. (Reproduced from G.E. Martin and A.S. Zektzer, *Two-Dimensional NMR Methods for Establishing Molecular Connectivity*, VCH, New York, 1988, p. 362.)

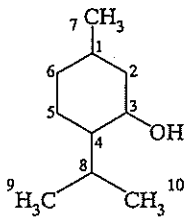

6-2

Figure 6-30 illustrates the 2D INADEQUATE spectrum of menthol **(6-2)**. The experiment also has been called C,C COSY, as the cross peaks represent connectivity between two carbons. There are no diagonal peaks, which would arise from ^{13}C nuclei with ^{12}C neighbors, because the experiment removes single quantum signals. The diagonal usually is drawn in, as in Figure 6-30. At the bottom is given the normal proton-decoupled ^{13}C spectrum. At the top the 2D procedure permits recovery of the carbon-coupled ^{13}C spectrum through a projection of the ν_2 dimension.

To obtain connectivity from a 2D INADEQUATE experiment, a single assignment is made and the remainder of the structure is mapped. Only a gap caused by the presence of a heteroatom, C—X—C, prevents mapping the entire skeleton. For menthol, the oxygen-substituted C-3 resonates at highest frequency (the far left). Horizontal lines are drawn between coupled carbons in the 2D spectrum (Figure 6-30), passing through the diagonal at their midpoints. There are two cross peaks at the C-3 frequency, corresponding to connectivities to C-2 and to C-4. Of these, the secondary C-2 should be at lower frequency (higher field). The connectivity then may be followed: C-2 ⟶ C-1 ⟶ C-6 (and from C-1 to the C-7 methyl) ⟶ C-5 ⟶ C-4 ⟶ C-8 (and from C-4 to the original C-3) ⟶ C-9 and C-10.

The major disadvantage to this experiment is its extremely low sensitivity. Although numerous technical refinements have been applied to 2D INADEQUATE to ameliorate this and other disadvantages, it is unlikely that the experiment will be widely used. Alternative connectivity experiments that utilize proton sensitivity through relay methods or inverse detection may be preferred.

6-5 HIGHER DIMENSIONS

The enormous complexity of spectra of large biomolecules such as proteins, polynucleotides, or polysaccharides has led to the development of three- and four-dimensional experiments. Two independently incremented evolution periods (t_1 and t_2) in conjunction with three separate Fourier transformations of these and the acquisition period t_3 result in a cube of data with three frequency coordinates.

From a study by van de Ven, Figure 6-31 illustrates the complexity of the 2D NOESY spectrum of a DNA-binding protein of phage Pf3, consisting of 78 amino acids. The vertical line at δ 9.35 highlights the problems at a single resonance position in the NH region. The NH proton in a given peptide unit —CHR'—CO—NH—CHR—CO— could have one cross peak with its own CHR proton and another with the neighboring CHR' protein, but the NOESY spectrum contains more than a dozen cross peaks at the one frequency at δ 9.35. Thus more than one NH must be generating cross peaks at this frequency.

The nitrogen HMQC experiment provides connectivity information about nitrogens and their attached protons. For proteins, use of HMQC normally requires isotopic enrichment of ^{15}N, which is obtained by growing an organism in a medium containing a single nitrogen source such as $^{15}NH_4Cl$ (similarly, ^{13}C enrichment may be obtained by use of a medium containing ^{13}C-labeled glucose). The normal 2D HMQC spectrum (^{15}N vs. ^{1}H) for this same protein is given in Figure 6-32, and two connectivities are seen

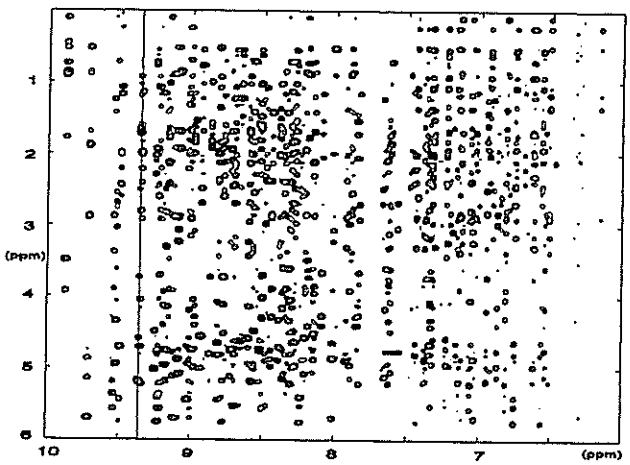

Figure 6-31 A portion of the NOESY spectrum of a DNA-binding protein of phage Pf3 containing cross peaks between NH and aliphatic protons. (Reproduced from F.J.M. van de Ven, *Multidimensional NMR in Liquids,* VCH, New York, 1995, p. 296.)

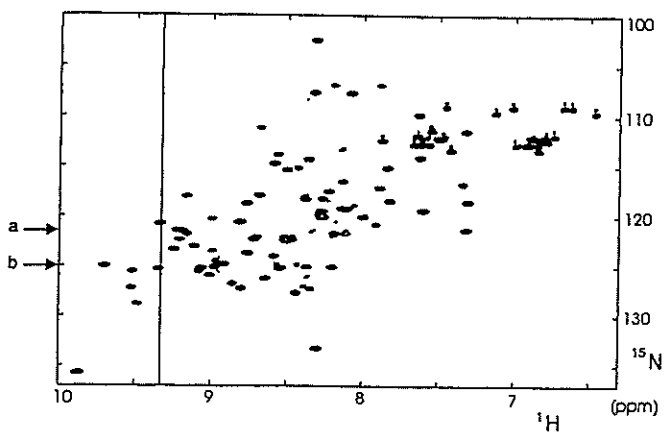

Figure 6-32 The ^{1}H,^{15}N HMQC spectrum of ^{15}N-labeled Pf3. The

at the ^{1}H frequency of δ 9.35 (vertical line). Thus there are two NH resonances (or more if there are coincidences) at δ 9.35.

The 3D experiment takes the 2D experiments in Figures 6-31 and 6-32 into an additional dimension. The 3D procedure illustrated in Figure 6-33 labels each NOESY peak with the ^{15}N frequency through the HMQC method, thus combining NOESY and HMQC data. The pulses and time delays comprise the standard NOESY sequence through the third 90° ^{1}H pulse. The pulses and delays thereafter are the standard HMQC sequence, which ends with inverse detection of ^{15}N at the ^{1}H frequencies in t_3. The totality of data requires a cube for representation, as diagrammatically in Figure 6-34, in which the flat dimensions are the NOESY data in ^{1}H frequencies and the vertical axis is the ^{15}N frequencies from HMQC. In practice, horizontal planes (single ^{15}N frequencies) are selected for analysis, as in Figure 6-35 for δ 120.7 and 124.9 (see the arrows labeled a and b in Figure 6-32). The vertical lines at δ 9.35 each show two dominant cross peaks for the NH NOEs to the inter- and intraresidue CHR. Note that both ^{15}N frequencies show a cross peak for δ 9.35 at a CHR frequency of δ 5.2, so that indeed there is overlap in Figure 6-32.

This type of heteronuclear 3D experiment is called NOESY–HMQC (in Figure 6-34 there are two ^{1}H dimensions and one ^{15}N dimension). Most 3D experiments use high-sensitivity methods and displays that are particularly effective for large molecules. Thus COSY is not often used, but TOCSY–HMQC is a useful method

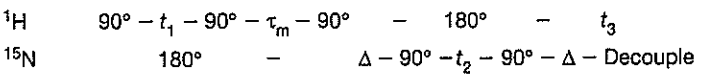

Figure 6-33

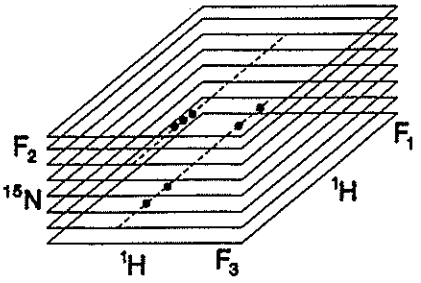

Figure 6-34 Diagram of the 3D ^{1}H,^{15}N NOESY–HMQC spectrum of Pf3 in three frequency dimensions: F_1, F_2, F_3 (ν_1, ν_2, ν_3). (Reproduced from F.J.M. van de Ven, *Multidimensional NMR in Liquids*, VCH, New York, 1995, p. 299.)

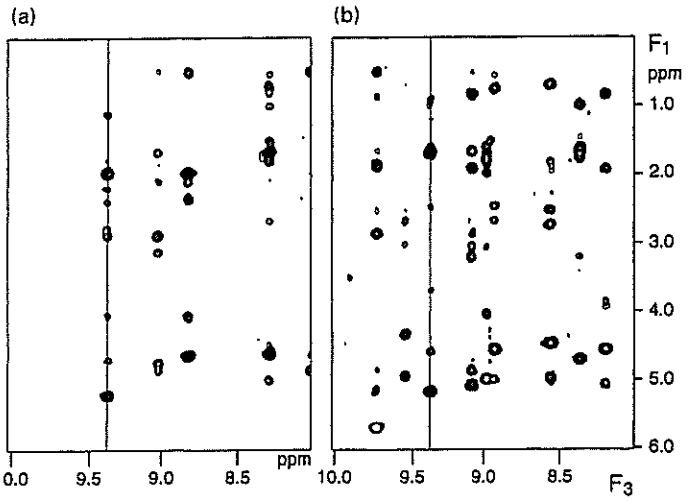

Figure 6-35 Two ν_1–ν_3 (F_1–F_3) planes taken from the 3D ^{1}H,^{15}N NOESY–HMQC spectrum of Pf3, corresponding to the frequencies indicated by arrows in Figure 6-32. (Reproduced from F.J.M. van de Ven, *Multidimensional NMR in Liquids*, VCH, New York, 1995, p. 300.)

to separate ^{1}H–^{1}H coupling connectivities into a ^{13}C or ^{15}N dimension. The homonuclear 3D experiment NOESY–TOCSY (all three dimensions are ^{1}H) separates through-space connectivities from coupling connectivities by the simple pulse sequence $90° - t_1 - 90° - \tau_m - t_2 - (\text{spin lock}) - t_3$. The three dimensions may each represent a different nuclide, as in ^{1}H/^{13}C/^{15}N, and are considered as variants of the HETCOR experiment. The nuclides usually are selected to explore specific connectivities in biomolecules. The H–N–CO experiment looks at the connection ^{1}H—^{15}N—(C)—^{13}C═O in the peptide unit —NH—CHR—CO— and requires double labeling of ^{15}N and ^{13}C to provide sufficient sensitivity in proteins. The 3D cross peaks connect the HN proton in the first dimension, the HN nitrogen in the second, and the intraresidue carbonyl carbon in the third. An analogue in nucleotide analysis is the H–C–P experiment, in which the third dimension is ^{31}P. Numerous variations of these triple resonance experiments exist. In particularly complex cases a fourth time domain t_4 may be introduced to produce 4D experiments.

These higher dimensions of NMR require a computer with powerful storage and graphics capabilities. When through-bond connectivity experiments are combined with the spatial information from buildup rates of NOESY cross peaks, proton–proton distances can be obtained by referencing to known bond lengths. The result can be the complete three-dimensional structure of biomolecules. Such solution-phase structures complement solid-phase information from X-ray crystallography. In this way, NMR spectroscopy has become a structural tool for obtaining detailed molecular geometries of complex molecules.

6-6 PULSED FIELD GRADIENTS

Field inhomogeneity has been mentioned as the primary contributor to transverse relaxation (T_2) (Sections 2-3 and 5-1). Transverse *(xy)* magnetization arises because the phases of individual magnetic vectors became coherent rather than random (respectively, Figures 2-10 and 2-11). In a perfectly homogeneous field, this coherence would relax only through spin–spin interactions. In an inhomogeneous field, however, the existence of slightly unequal Larmor frequencies permits vectors to move faster or more slowly than the average, thereby randomizing their phases and destroying transverse magnetization, as described in Section 2-3.

There are several instances in which transverse magnetization is unwanted and may be eliminated by application of a pulsed field gradient (PFG) (also called a gradient pulse). An example of a PFG is illustrated in Figure 6-36. This gradient is along the direction *(z)* of the B_0 field. On application, nuclei with different positions in the sample (different z coordinates) resonate at different frequencies. Such spatial encoding of frequency information is the fundamental principle of magnetic resonance imaging (MRI). For the present context, it may be viewed as a method for inducing transverse relaxation very quickly by rapid dephasing. In a typical 2D pulse sequence, a delay time is necessary between repetitions of the pulse sequence in order for relaxation to occur. If repetition occurs before transverse magnetization has relaxed to zero, artifacts may occur in the 2D spectrum. Consequently, application of a PFG at the beginning of the sequence avoids this problem. For the NOESY experiment, the following pulse sequence may be used: $\text{G1} - 90° - t_1 - 90° - \tau_m$, $\text{G2} - 90° - t_2$.

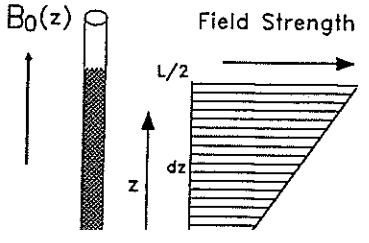

Figure 6-36 Diagram of a B_0 field gradient along the z direction. (Reproduced from

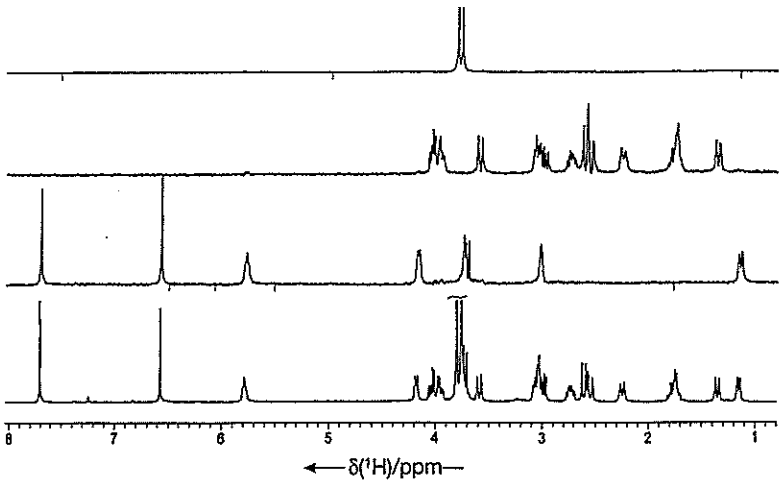

Figure 6-37 Editing of the ^{1}H spectrum of brucine **(6-3)** into subspectra for CH_3, CH_2, and CH (top to bottom). The complete ^{1}H spectrum is given at the bottom. (Reproduced with permission from T. Parella, F. Sánchez-Ferrando, and A. Virgili, *J. Magn. Reson. A*, **117**, 80 [1995]).

The first PFG (G1) destroys residual transverse magnetization from prior pulses by dephasing the magnetic vectors. A second PFG (G2) is applied during the mixing period τ_m. Only the effects on longitudinal *(z)* magnetization are of interest during this period. Application of the PFG eliminates false cross peaks that can arise from transverse magnetization.

In addition to dephasing transverse magnetization, PFGs are used to select coherence order. Use of phase cycling to select coherence order inevitably involves multiple scans, by which pulse sequences move through 4 or 16 or 64 variations with switching of x, $-x$, y, and $-y$, for example. Full exploitation of phase cycling thus is time consuming. The development of zero, single, or double quantum coherence depends on the rate of various dephasing processes. Proper use of PFGs permits selection of coherence order without the repetitive scans of phase cycling. For example, in the inverse detection HETCOR experiment, the single quantum coherence signal for protons attached to ^{12}C (or ^{14}N) must be suppressed while selecting the double quantum coherence signal for protons attached to ^{13}C (or ^{15}N). By phase cycling, this selection is achieved by measuring the difference between two strong signals. The PFG method selects and measures the small signal directly in a single scan.

PFG procedures have been developed to implement most of the 1D and 2D experiments discussed in the last two chapters. They may be used for solvent suppression, INADEQUATE, all common 2D experiments, and spectral editing. A PFG combination of DEPT and HMQC results in editing of proton spectra according to carbon substitution patterns. A PFG-based multiple quantum filtration leads to evolution of double, triple, or quadruple quantum coherence, respectively leading to proton spectra containing only CH, CH_2, or CH_3 resonances. Broadband decoupling removes coupling to ^{13}C, while proton-proton couplings remain. Figure 6-37 illustrates the result for brucine **(6-3)**.

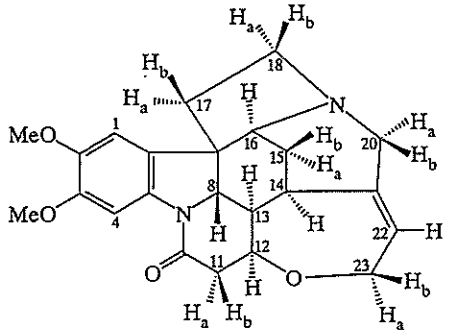

6-3

6-7 SUMMARY OF TWO-DIMENSIONAL METHODS

There is a bewildering array of two-dimensional methods available to the NMR spectroscopist today. This chapter has described a number of the most widely used experiments. A routine structural assignment begins with recording the one-dimensional ^1H and ^{13}C spectra. Many resonances may be assigned according to the principles outlined in Chapters 3 and 4 on chemical shifts and coupling constants. Normally recourse is made to 2D methods only if this traditional approach is insufficient. Some type of spectral editing for determining the number of protons attached to each carbon, such as DEPT, is helpful in completing the ^{13}C assignments (Section 5-5). The HETCOR experiment then provides correlations between the ^{13}C and ^1H resonances, possibly with completion of the ^1H assignments.

Further 2D methods are necessary if the structure is not solved in the process of making spectral assignments for hypothetical or expected structures. The COSY experiment lays the groundwork for structure determination through ^1H–^1H connectivities based on J couplings. For small molecules, there may not be enough vicinal or geminal couplings for the method to be useful. For molecules of medium complexity, COSY may be sufficient to provide the entire structure by confirming expected ^1H–^1H connectivities based on vicinal and geminal couplings. The analogous experiment based on long range couplings (LRCOSY) may be necessary to assign connections between molecular pieces that do not involve vicinal protons, for example between two rings, for substituents on a ring, or over a heteroatom or carbonyl group.

Additional 2D experiments may be necessary for larger molecules. As peaks accumulate along the diagonal, the COSY45 or DQF–COSY experiment may be used to simplify that region and uncover cross peaks that are close to the diagonal. For even larger molecules, the TOCSY or relayed COSY experiments may be necessary. Further connectivities between protons and carbons may be explored through long range couplings (COLOC). The HMQC experiment may replace HETCOR if higher sensitivity is required or if ^1H–^{13}C couplings are needed. If ^1H–^1H couplings need to be measured, either the J-resolved method or phase sensitive COSY may be carried out.

The NOESY experiment provides information about the proximity of protons and hence is used primarily for distinguishing structures that have clear stereochemical differences. For larger molecules the ROESY experiment may offer some advantages because of its lower tendency to exhibit spin diffusion. The related EXSY experiment is used only when chemical exchange is being investigated.

The 2D INADEQUATE experiment requires additional spectrometer time. It may be an experiment of last resort, although specific structures may be particularly amenable to this technique, as for example when there are several quaternary carbons that prevent COSY analysis.

For a large selection of relatively straightforward 2D spectra, refer to the early examples of the Integrated Problems (see Chapter 16). The following problems involve molecules of medium to high complexity, although none is so complex as to require 3D methods.

6-1 Below is the 300 MHz COSY spectrum* of a molecule with the formula $C_{14}H_{20}O_2$. The 1D spectrum is given on either edge. In addition to the illustrated resonances, the ^1H spectrum contains a broad singlet at δ 7.3 with integral 5. What is the structure? Show your reasoning.

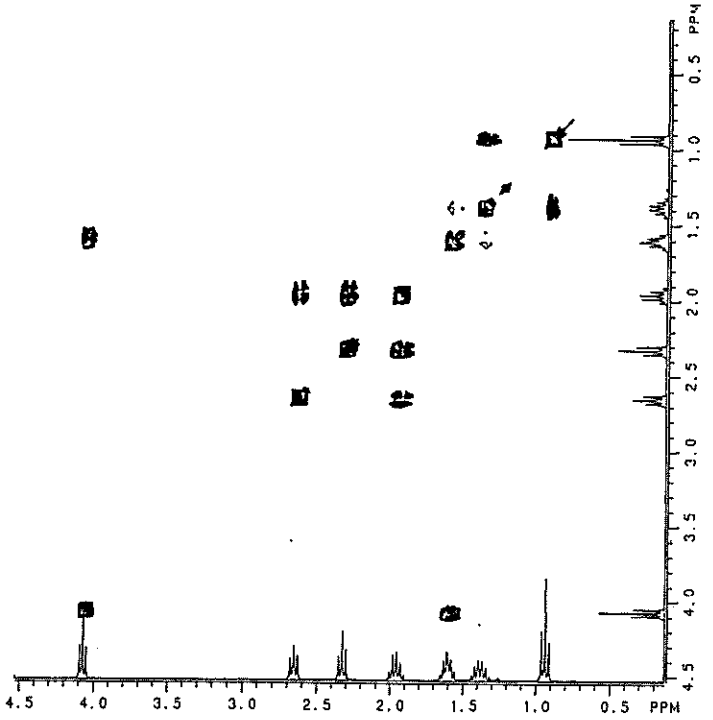

6-2 The trimerization of indole-5-carboxylic acid gives one of the following two isomers.

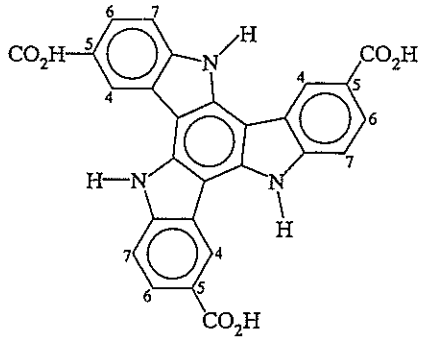

I

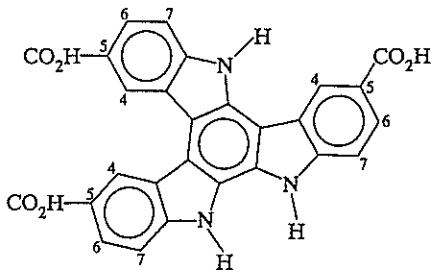

II

On the following page are the 360.1 MHz ^1H spectrum† of the product and the COSY spectrum (with a blow-up of the δ 7.8–8.2 region) in DMSO-d_6. The signal marked * is an impurity. The ^1H signals are labeled A to N. Signals A to D were removed with the addition of D_2O. Signal A is a broad peak at the base of B. The following 1D NOE results were obtained. Irradiation of B affected F/G and N. Irradiation of C and D affected M and L, respectively. Irradiation of F/G affected B.

*Reproduced with permission from S.E. Branz, R.G. Miele, R.K. Okuda, and D.A. Straus, *J. Chem. Educ.*, **72**, 659-661 (1995). Copyright 1995 American Chemical Society.

†J.G. Mackintosh, A.R. Mount, and D. Reed, *Magn. Reson. Chem.*, **32**, 559-560 (1994). Reproduced with permission from John Wiley & Sons Ltd.

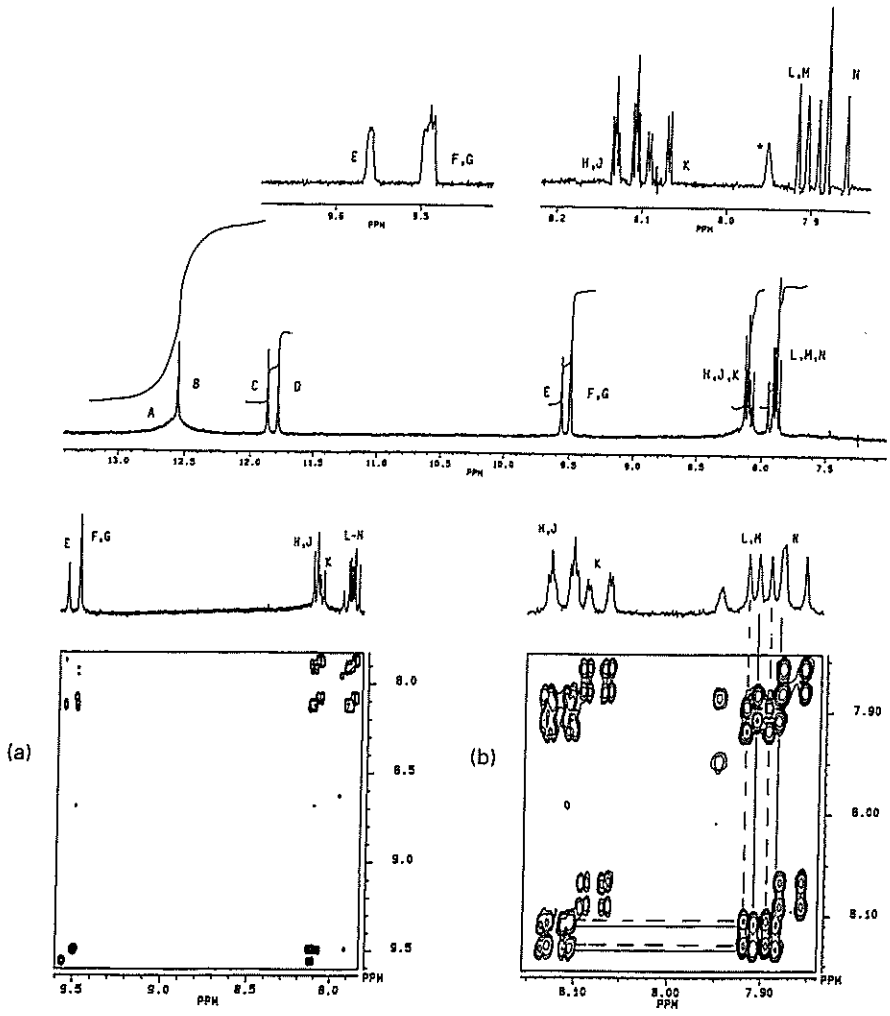

(a) From the overall appearance of the spectrum, is the trimer I or II? Explain.

(b) Using peak multiplicities, the NOE experiments, and the COSY spectrum, assign all the resonances. Discuss your reasoning in a step-by-step fashion. You should end up with an assignment of peaks A to N to specific protons.

6-3 The 500 MHz ^1H spectrum of the illustrated sugar derivative (extracted from a bean) is given below, aside from hydroxy resonances.

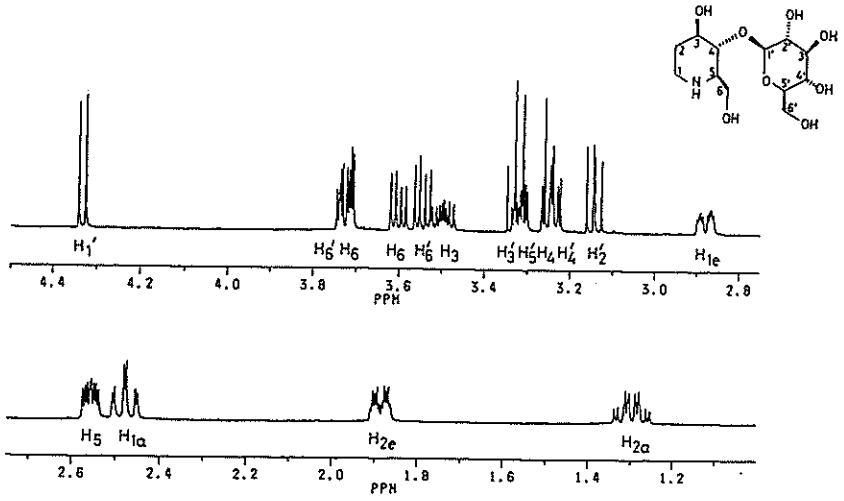

(a) The complete COSY spectrum* is given below with the assignment of one resonance. Complete the assignment for protons in the sugar ring.

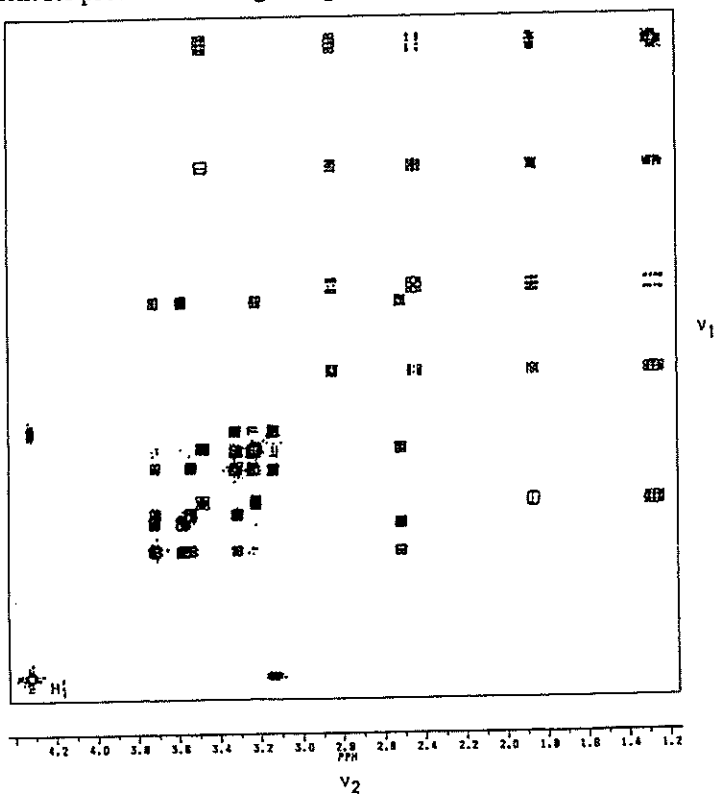

(b) A slightly expanded version of the low-frequency portion of the COSY spectrum is given below, again with the assignment of one resonance. Complete the assignment for the protons of the piperidine ring. First, it is advisable to draw out the chair conformation.

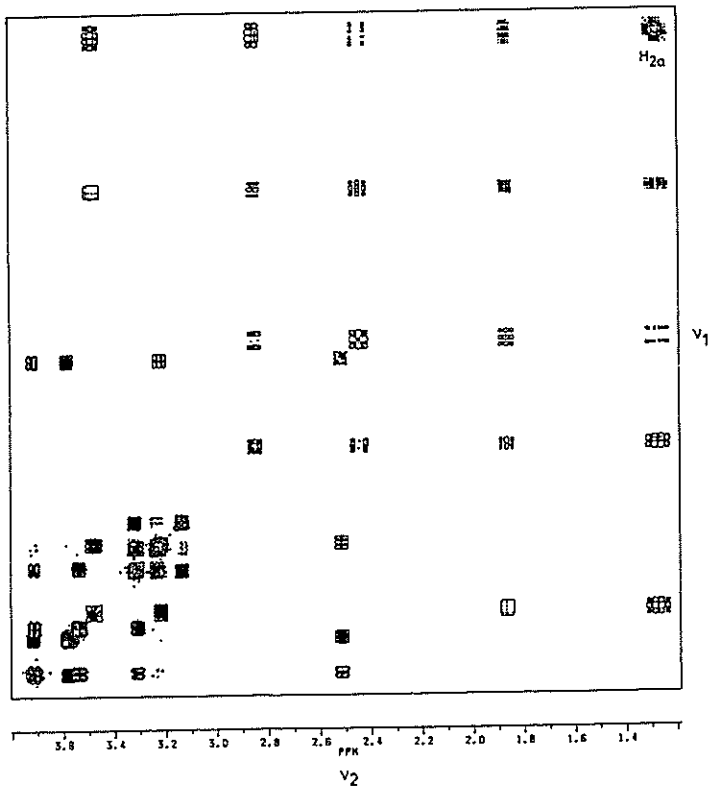

*A.E. Derome, *Modern NMR Techniques for Chemistry Research,* Pergamon Press, Oxford, UK, 1987, pp. 191-194.

6-4 Given below is the 600 MHz COSY45 spectrum* for a mixture of 3-*endo*- and 3-*exo*-fluorocamphor. The two high-frequency peaks are from the 3 protons respectively on the exo-F isomer ("3n," an endo proton) and the endo-F isomer ("3x," an exo proton). The remaining protons have been assigned to position but not to isomer. Using the COSY45 spectrum, indicate which peaks come from the exo and which from the endo isomer. Show your reasoning by drawing lines on the spectrum.

6-5 **(a)** From the following 300 MHz ^{1}H spectrum† of phenanthro[3,4-b]thiophene, identify the resonances of H-1 and H-11, as a pair. How are these distinguished from the remaining resonances?

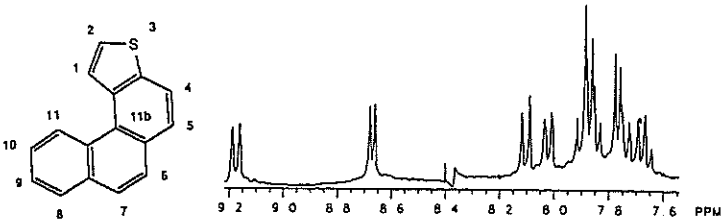

(b) From the 300 MHz COSY spectrum† given below, how would you distinguish H-1 and H-11? Assign resonances to H-2, H-8, H-9, and H-10.

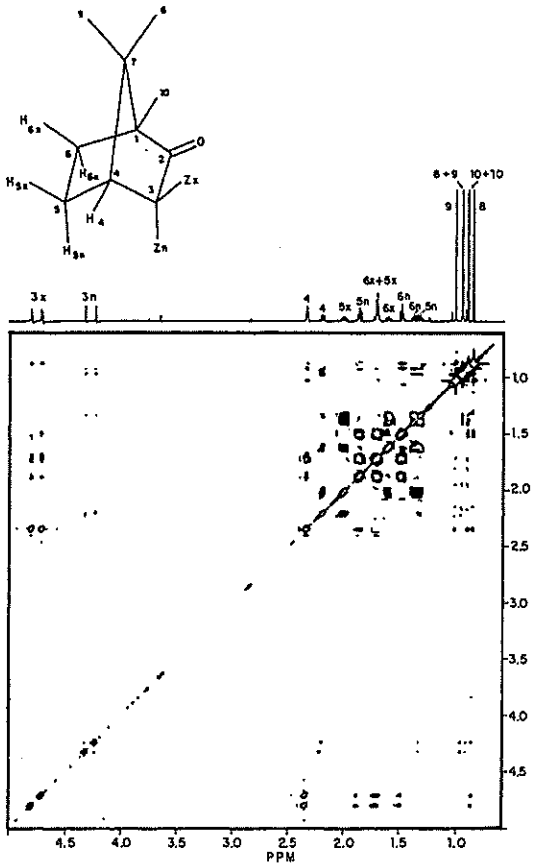

COSY45 Spectrum for Problem 6-4

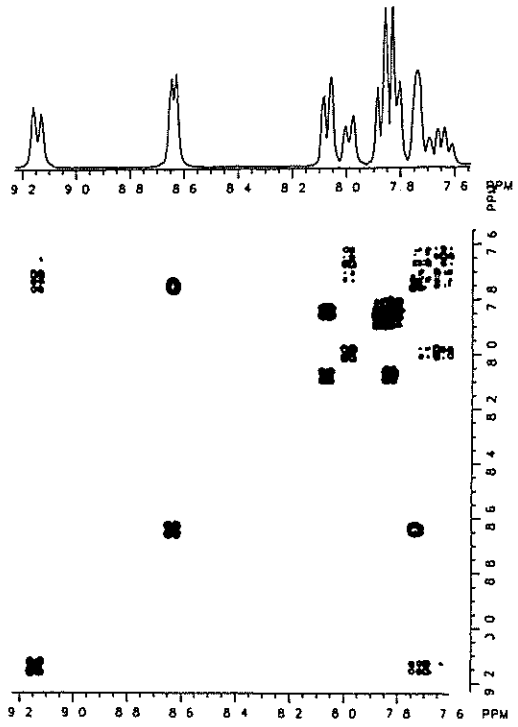

COSY Spectrum for Problem 6-5b

*C.R. Kaiser, R. Rittner, and E.A. Basso, *Magn. Reson. Chem.*, **32**, 503-508 (1994). Reproduced with permission of John Wiley & Sons Ltd.

†Reproduced from G.E. Martin and A.S. Zektzer, *Two-Dimensional NMR Methods for Establishing Connectivity,* VCH, New York, 1988, pp. 75-78.

6-6 With only the 2D INADEQUATE carbon spectrum* given below, derive the structure of the unknown. You will have to suggest a functionality attached to the highest frequency carbon, marked with an **a** in the spectrum.

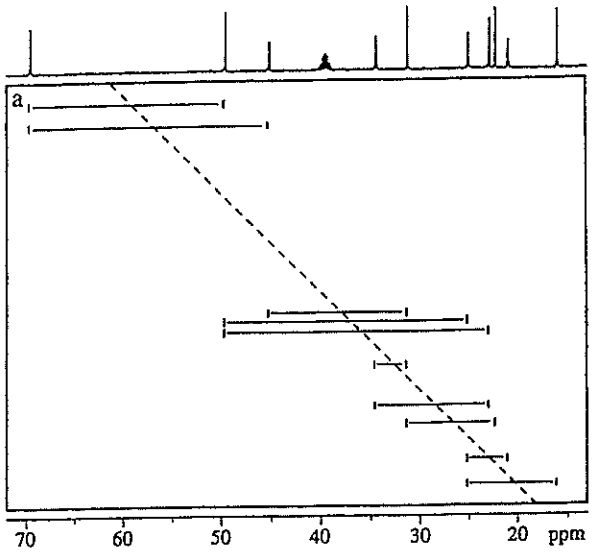

6-7 Upjohn scientists isolated a potent inhibitor of the cholesteryl ester transfer protein, U-106305. The high-resolution mass spectrum indicated the formula to be $C_{28}H_{41}NO$, and the ^{13}C spectrum had 27 distinct resonances (including one pair of equivalent carbons at δ 20.02). DEPT spectra indicated the multiplicities given in the table below.

(a) The infrared spectrum showed intense bands at 1630 and 1558 cm^{-1}. What functional group is suggested? What NMR peak confirms this assignment?

(b) What substructures are suggested by the ^{13}C peaks at δ 120–150?

(c) The HETCOR spectrum gave full ^1H assignments (see table below). From the ^1H resonance correlated with the δ 120–150 ^{13}C peaks, what else can you tell about the substructures from **(b)**? Use the magnitudes of *J* (values in parentheses), the values of the four ^1H and ^{13}C chemical shifts, and the proton multiplicities. In particular, note that δ 120 is d rather than dd.

(d) The UV–vis spectrum showed a strong band at 215 nm. Using the functional groups you have already deduced, what is the chromophore?

(e) Note the six low-frequency ^{13}C triplets. Each is correlated with a very low frequency (high field) pair of protons ($\delta < 0.7$). What grouping is suggested here that is present six times?

*Reproduced with permission from N.C. Nielsen, H. Thøgersen, and O.W. Sørensen, *J. Am. Chem. Soc.*, **117**, 11365-11366 (1995). Copyright 1995 American Chemical Society.

^{13}C Chemical Shift and Multiplicities	*^1H Chemical Shift and Coupling Constants*	*^{13}C Chemical Shift and Multiplicities*	*^1H Chemical Shift and Coupling Constants*
7.6 (T)	0.07, 0.09 (dt: 8.43, 4.85)	20.0 (D)	1.00 (m)
7.6 (T)	0.12, 0.16 (dt: 8.39, 4.90)	20.02 (Q)	0.90 (d: 6.8)
8.0 (T)	0.08 (not first order)	20.7 (D)	1.29 (m)
11.4 (T)	0.32, 0.34 (dt: 8.20, 4.77)	21.8 (D)	0.68 (m)
13.4 (T)	0.65 (dt: 8.59, 4.87)	22.4 (D)	0.94 (m)
14.8 (T)	0.34, 0.43 (dt: 8.33, 4.60)	24.0 (D)	1.01 (m)
14.8 (D)	0.63 (m)	28.5 (D)	1.77 (h: 6.8)
17.9 (D)	0.57 (dq: 13.27, 4.93)	46.7 (T)	3.20 (d: 6.8)
18.0 (D)	0.58 (m)	120.0 (D)	5.91 (d: 15.2)
18.2 (D)	0.49 (m)	130.4 (D)	4.98 (dd: 15.5, 7.2)
18.2 (D)	0.51 (m)	131.0 (D)	4.98 (dd: 15.5, 7.7)
18.4 (D)	0.53 (m)	148.8 (D)	6.24 (dd: 15.2, 9.8)
18.41 (Q)	1.02 (d: 6.0)	166.0 (S)	
18.8 (D)	0.60 (m)		

(f) Now count up your unsaturations. You should have accounted for them all. Enumerate them.

(g) The DQF–COSY spectrum was given by the authors for one substructure as follows: the integral-6 ^{1}H resonance at δ 0.90 (d: 6.8) was linked to the integral-1 resonance at 1.77 (heptet: 6.8), which was linked to the integral-2 resonance at δ 3.20 (d: 6.8). What substructure is suggested by this 2D evidence?

(h) How is this substructure linked to a previously determined functionality? Look at the chemical shifts.

(i) You actually have almost all the structure now. The remaining unassigned ^{13}C resonances are twelve doublets and one quartet. Locate these carbons (without specific assignment) on your previous substructures and comment on the chemical shifts of the attached protons.

(j) These protons are all found in the DQF–COSY spectrum, except for the δ 1.29 resonance. Even at 600 MHz, there is severe overlap, so here are the connectivities derived from this experiment.

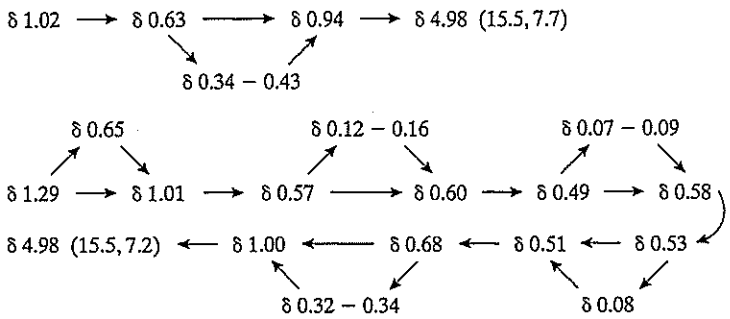

Write out the entire structure. Some stereochemistries are not set.

(k) Look at the available multiplicities and J values for the protons associated with the six high frequency triplets (all are dt with J either ~8.4 or ~4.8 Hz). This information sets the final stereochemistries. Give the full structure.

BIBLIOGRAPHY

Also see general texts referenced in previous chapters.

6.1. R.R. Ernst, G. Bodenhausen, and A. Wokaun, *Principles of Nuclear Magnetic Resonance in One and Two Dimensions,* Oxford University Press, Oxford, UK, 1987.

6.2. G.E. Martin and A.S. Zektzer, *Two-Dimensional NMR Methods for Establishing Molecular Connectivity,* VCH, New York, 1988.

6.3. K. Nakanishi, *One-Dimensional and Two-Dimensional NMR Spectra by Modern Pulse Techniques,* University Science Books, Mill Valley, CA, 1990.

6.4. *Two-Dimensional NMR Spectroscopy,* R.R. Croasmun and R.M.K. Carlson, eds., 1st and 2nd ed., VCH, New York, 1987, 1994.

6.5. H. Friebolin, *Basic One- and Two-Dimensional NMR Spectroscopy,* VCH, Weinheim, Germany, 1993.

6.6. F.J.M. van de Ven, *Multidimensional NMR in Liquids,* VCH, New York, 1995.

6.7. J.N.S. Evans, *Biomolecular NMR Spectroscopy,* Oxford University Press, Oxford, UK, 1995.

6.8. Atta-ur-Rahman and M.I. Choudhary, *Solving Problems with NMR Spectroscopy,* Academic Press, San Diego, CA, 1996.

6.9. COSY: A. Kumar, *Bull. Magn. Reson.,* **10,** 96-118 (1988).

6.10. Long-range HETCOR: G.E. Martin and A.S. Zektzer, *Magn. Reson. Chem.,* **26,** 631-652 (1990).

6.11. EXSY: R. Willen, *Progr. NMR Spectrosc.,* **20,** 1-94 (1987); C.L. Perrin and T.J. Dwyer, *Chem. Rev.,* **90,** 935-967 (1990).

6.12. Multiple quantum methods: T.J. Norwood, *Progr. NMR Spectrosc.,* **24,** 295-375 (1992).

6.13. Composite pulses: M.H. Levitt, *Progr. NMR Spectrosc.,* **18,** 61-122 (1986).

6.14. Pulsed field gradients: W.S. Price, *Ann. Rev. NMR Spectrosc.,* **32,** 51-142 (1996); T. Parella, *Magn. Reson. Chem.,* **34,** 329-347 (1996).